POLITEHNICA UNIVERSITY TIMIŞOARA
Civil Engineering Faculty
Department of Steel Structures and Structural Mechanics

NUMERICAL MODELING OF MEMBRANE ACTION IN COMPOSITE SLAB WITH CELLULAR BEAMS IN FIRE

Author: Yuriy IZBASH, Civil. Eng.

Supervisor: Professor Raul ZAHARIA, Ph.D.

Universitatea Politehnica Timişoara, Romania

Study Program: **SUSCOS_M**

Academic year: **2014/2015**

MEMBERS OF THE JURY

President:

Professor Dan DUBINA, Ph.D.
C. M. of the Romanian Academy
Politehnica University Timişoara
Str. Ion Curea, Nr. 1
300224, Timisoara – Romania

Members:

Professor Raul ZAHARIA, Ph.D.
(Thesis Supervisor)
Politehnica University Timişoara
Str. Ion Curea, Nr. 1
300224, Timisoara – Romania

Professor Viorel UNGURIANU, Ph.D.
Politehnica University Timişoara
Str. Ion Curea, Nr. 1
300224, Timisoara – Romania

Assoc. Professor Adrian CIUTINA, Ph.D.
Politehnica University Timişoara
Str. Ion Curea, Nr. 1
300224, Timisoara – Romania

Secretary:

Assoc. Professor Adrian Dogariu, Ph.D.
Politehnica University Timişoara
Str. Ion Curea, Nr. 1
300224, Timisoara – Romania

ACKNOWLEDGMENT

I am grateful to my supervisor, Professor Raul ZAHARIA, Ph.D., for his guidance, encouragement and support throughout this research work.

My sincere thanks to Prof. ing. František WALD, Professor Dan DUBINA, Ph.D., Prof. dr. Luís Simões da Silva, Prof. dr. Jean-Pierre JASPART, Prof. dr. R. Landolfo and Prof. dr. Milan Veljkovic as coordinators of our SUSCOS_M European Erasmus Mundus Master program (Sustainable Constructions under natural hazards and catastrophic events 520121-1-2011-1-CZ-ERA MUNDUS-EMMC), for organizing this excellent master degree program and for their assistance and guidance.

I would like to thank Dr. Dan PINTEA and Dr. Cristian VULCU, for their patient guidance, encouragement and helpful advices.

Also, I grateful to my beloved family and friends, for their moral support, motivation and encouragement during my studies within this master course.

Finally, I would like to acknowledge the European Union, namely the Erasmus Mundus Scholarship, as without this funding I would not have the opportunity to participate in this master degree course.

ABSTRACT

The numerical work performed within this thesis is based on a full-scale fire test performed on a composite steel-concrete slab with cellular beams, made at the University of Ulster, U.K., within RFCS-FICEB Research Grant.

The numerical simulations were performed with the special purpose software SAFIR, dedicated to the structural analysis of structures under elevated temperatures. The numerical study contains several assumptions obtained from previous researches on modeling similar composite structures under ISO fire (FRACOF and COSSFIRE).

The aim of this work was to get results, which could describe the behavior of the tested structure as close as possible, while keeping a simplified numerical model, prone to be used in the design practice of such structures subjected to fire.

ORGANIZATION OF THE PRESENT THESIS

Chapter 1. Introduction

Describe the reasons of numerical simulation of the full-scale fire tests.

Chapter 2. FRACOF and COSSFIRE tests

Describe previously conducted tests on composite structures under ISO fire and assumptions used for their simulation.

Chapter 3. FICEB test

Describe parameters and conditions of the full-scale natural fire test.

Chapter 4. Numerical simulation

Describe the process and nuances of modeling composite slab with cellular beams under natural fire using SAFIR 2007 software.

Chapter 5. Results of the numerical simulation

Describe numerical simulations of composite slab with cellular beams under natural fire using different assumptions in order to increase model's behavior accuracy and keep it as simple as possible.

CONTENTS

FIGURES AND TABLES

CHAPTER 1. INTRODUCTION

1. INTRODUCTION

As spans become longer, steel framed constructions become more competitive compared with reinforced concrete structures. For maximum economy, steel beams should be designed to act compositely with the floor slab. The increased use of long span composite beams leads to large open area offices with minimal columns. However, as the span increases, the necessary beam depth will also increase that, in turn, can lead to increased story heights and the whole building itself. The use of cellular beams (CB) largely overcomes this problem because ducts, pipes and other services can pass through the openings in the web. Also, as CB is constructed from rolled sections, the increased section depth results in added strength without additional material use and consequently tends to reduce of the total weight of steelwork.

Membrane effect of partially protected composite steel-concrete slabs in fire situation was intensively studied since the first large fire tests performed at Cardington, UK (SCI, 1999), (Wang, 1996), which emphasized this particular structural behavior. A design method already exists (Bailey, 2001 and 2004), (Bailey et al., 2003), prone to be implemented in the futures Eurocodes for fire design.

However, an advanced numerical analysis using appropriate software for structural analysis under elevated temperatures may be required in particular situations. A complete and detailed numerical 3D model of a composite slab is too complex and time consuming to be performed in the current design practice, due to the simultaneous presence of beams and of orthotropic shells. Therefore, it is of interest to derive models as simple as possible that, based on approximations, would nevertheless yield an appropriate representation of the structural behavior and a safe estimation of the load bearing capacity.

The thesis investigates the ability of such a simplified model to reproduce the results of a natural fire test on a partially protected composite slab with cellular beams performed at University of Ulster within FICEB project (MACS+, RFCS, 2014), (Vasart and Zhao, ECCS, 2013), (FICEB, RFCS, 2012). The numerical analyses have been performed with the advanced calculation model SAFIR.

The numerical model was based also on the experience obtained on numerical simulations on similar slabs tested under ISO fire, with solid steel beams, FRACOF and COSSFIRE (Zaharia et al., 2013), (Vulcu et al., 2010)and on a previous simulation of the FICEB natural fire test (MACS+, RFCS, 2014), (Vasart and Zhao, ECCS, 2013), (FICEB, RFCS, 2012).

CHAPTER 2. FRACOF AND COSSFIRE TESTS

2.1 FRACOF - TEST DESCRIPTION AND PREVIOUS NUMERICAL SIMULATION WITH SAFIR

A typical composite steel-concrete slab, shown in Fig. 2.1 (Zhao et al. 2008), was adopted for this test.

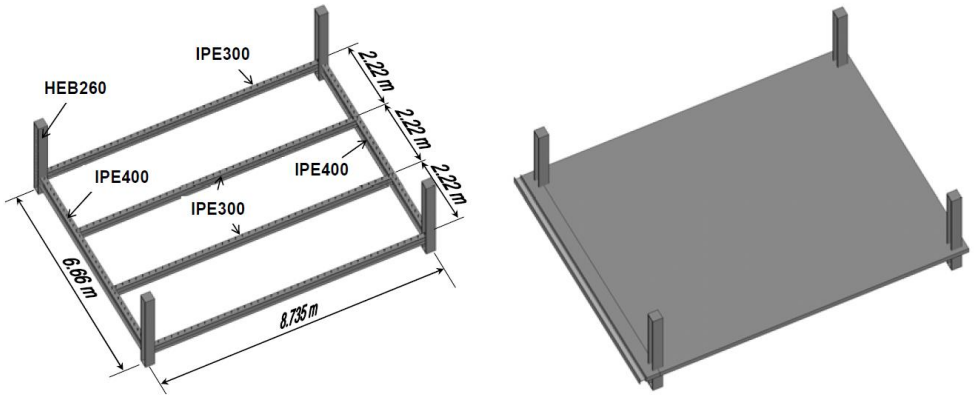

Fig. 2.1. Tested structure (Zhao et al. 2008)

The slab of the designed test specimen covered an area of 7.35m by 9.53m, laid on 6.66m by 8.735m steel structure. The slab comprised four secondary beams, two primary beams, four short columns and a 155mm thick floor slab realized with trapezoidal steel sheet of 0.75mm thickness (height of the ribs of 58mm). Normal weight concrete C30/37 was adopted in the design.

The reinforcing steel mesh of 7 mm used in the slab was realized with S500 steel grade and had a grid size of 150 × 150 mm. The axis distance of the steel reinforcement from top of the slab was 50 mm. S235 steel grade was used for secondary beams and S355 for main beams. All steel beams were linked to the concrete slab with the help of headed studs, and to the columns with two common types of steel joints (flexible end plate and double angle web cleats).

During the fire test, the mechanical loading of the floor was applied using fifteen sand bags distributed over the floor leading to an equivalent uniform load

of 3.87 kN/m². The two secondary beams and the composite floor were unprotected, while all the edge beams of the floor, namely all beams in direct connection with columns, were fire protected with fiber-based insulation to ensure a global structural stability under fire situations. The ISO fire exposure lasted up to 123 minutes.

The numerical analysis described further was performed by Zaharia et al, 2013. The properties of the insulation material that have been used in the simulation were the nominal ones (those given by the producer). The variation of the thermal conductivity, thermal elongation and specific heat of steel function of temperature was considered as given in EN 1993-1-2 (2005). A siliceous type of concrete was considered. The upper limit of the thermal conductivity according to EN 1992-1-2 (2005) was considered for concrete. Other parameters considered for the concrete within the composite slab are: 2400 kg/m^3 specific mass, 46 kg/m^3 water content and 0.7 surface emissivity. Due to the ISO fire exposure, for all materials, the convection coefficient on heated surfaces was considered 25 W/m^{2}K, while the convection coefficient on unheated surfaces was 9 W/m^{2}K.

For the unprotected beams, the fire exposure was considered on three sides (without the top flange). In the structural analyses, only the concrete located above the trapezoidal sheets has load-bearing capabilities.

However, the presence of the ribs is important for the temperature distribution in the concrete and in the rebars. For the thermal distribution, in order to obtain a simple numerical model, the cross section of the slab containing ribs has been replaced by a section with an equivalent thickness calculated according to EN1994-1-2. Annex D (2005).

The slab cross-section model was thus selected after comparing four different cases, see Fig. 2.2 (Vulcu, 2009):

1) Real shape composite slab without steel deck;

2) Real shape composite slab with steel deck;

3) Real shape composite slab with the gap between steel and concrete;

4) Effective thickness of the slab only with concrete.

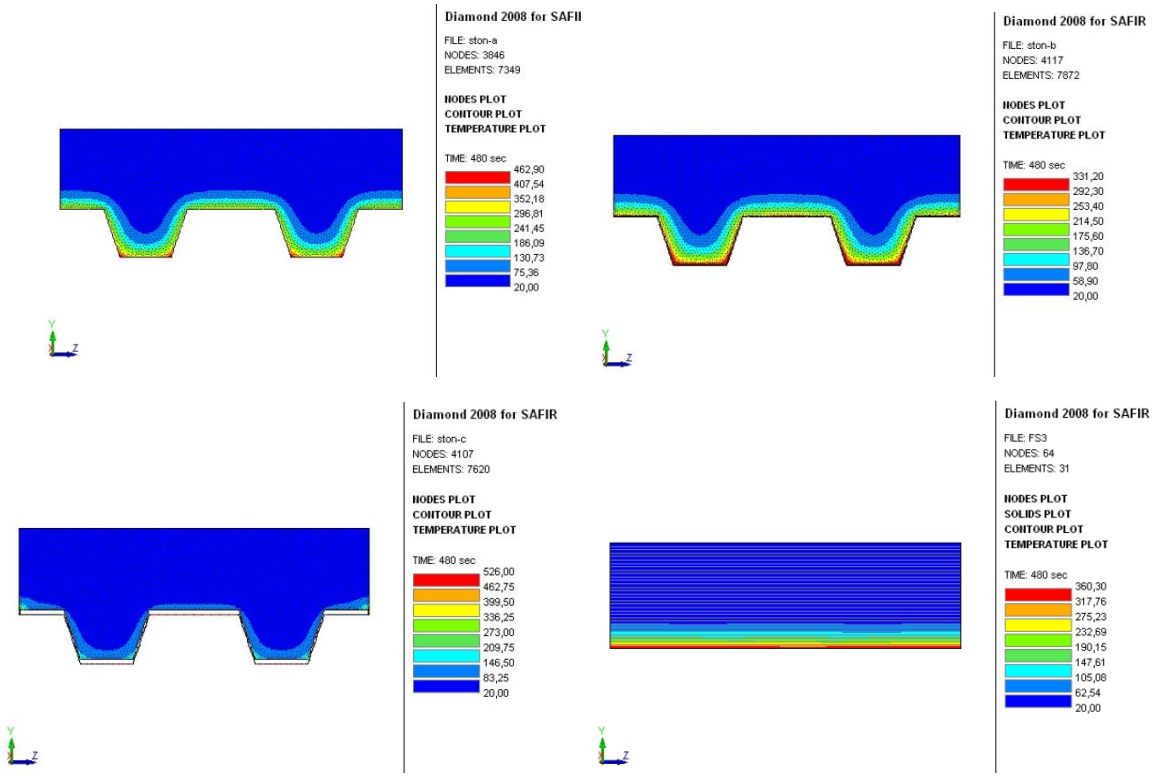

Fig. 2.2. Effective thickness Vs real shape of the slab (Vulcu, 2009)

From the comparison presented in Fig. 2.3, it is clear that the influence of the steel deck is very small on the thermal distribution of element, the two upper time-temperature curves being identical. In case of void between concrete and steel deck, temperatures are lower than in the previous cases and closer to the measured one, and for an effective thickness of the slab, the time-temperature curve is even closer to the real one. Because of these facts, in the FICEB simulation it was used the fourth type of section for the idealization of the

composite slab. In addition, it consumes less time on calculation due to simple shape.

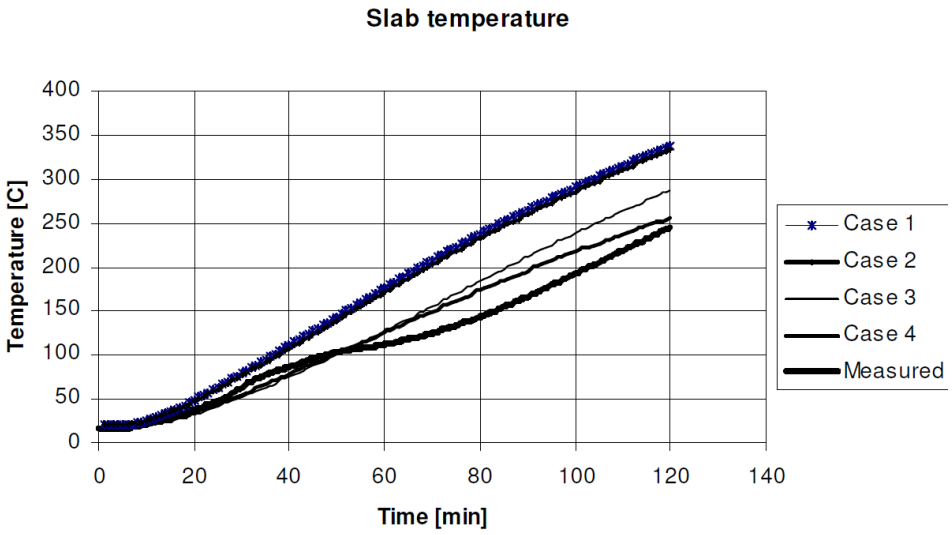

Fig. 2.3. Temperature comparison for different types of slab (Vulcu, 2009)

The primary and secondary beams have been idealized using beam elements, and the slab using shell elements. For the structural analysis, only the concrete that is present above the corrugated steel profiles was considered, while the concrete underneath only forms a thermal protection equivalent to the protective effect of the ribs. According to the joints details from the test, the beam-to-column and beam-to-beam connections were modelled as pinned. The rebars have been modelled as an equivalent steel layer on the thickness of the shell element. Even though at the test the load was "concentrated" by using sand bags, in the simulation the load was considered uniformly distributed. For the material properties, the nominal values have been used, not the measured ones.

In Fig. 2.4, the calculated deformed shape and the membrane stresses of the slab are shown, at 165 minutes. At this moment, in the simulation, the structure failed due to large deflections of the secondary edge beams. The membrane action, characterized by the equilibrium between the compression of

the concrete on the edges of the slab and the tension in the rebars from the middle of the slab, was overreached, and the slab could not uphold the load any longer. The chart shows the comparison between the measured and the calculated deflection at the center of the slab.

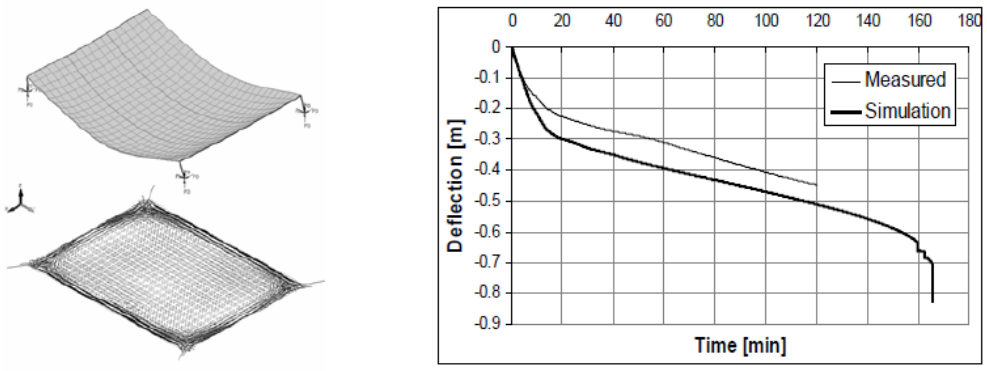

Fig. 2.4. Deformed shape and membrane forces – Deflection in the middle of the slab (Zaharia et al, 2013)

2.2 COSSFIRE – TEST DESCRIPTION AND SAFIR NUMERICAL SIMULATION

The concrete slab covered an area of 6.66m by 8.5 m, as shown in Figure 2.5 (COSSFIRE, 2006).

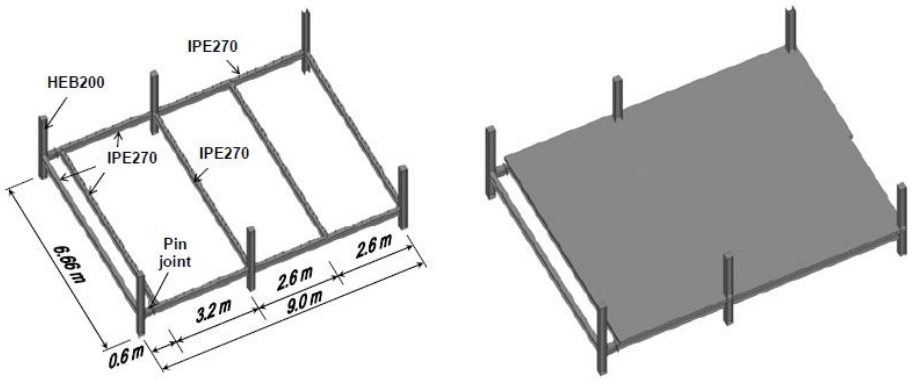

Fig. 2.5. Tested structure (COSSFIRE, 2006)

The composite steel and concrete floor was made of five secondary beams, four primary beams, six short columns and a 135 mm thick slab realized with trapezoidal steel sheet of 0.75 mm thickness (height of the ribs of 58 mm). Normal weight concrete C30/37 was adopted in the design.

The reinforcing steel mesh with 8 mm diameter used in the slab was realized of S500 steel grade and had a grid size of 200 × 200 mm. The axis distance of the steel reinforcement from the top of the slab was 35 mm. As in case of the FRACOF test, the steel beams were linked to the concrete slab with help of headed studs, and to the columns with flexible end plate and double angle web cleats.

During the fire test, the mechanical loading of the floor was applied using sand bags, distributed over the floor, leading to an equivalent uniform load of 3.75 kN/m^2. The interior secondary beams and the composite slab were unprotected. All the boundary beams of the floor were fire protected by fiber-based insulation, in order to ensure a global structural stability under fire situations. As for the FRACOF test, the ISO fire exposure was stopped after 123 minutes.

The numerical analysis described further was also performed by Zaharia et al, 2009. The protected beams were placed on the edges, leading to a fire exposure on two sides. For the unprotected secondary beams, the fire exposure was considered on three sides, as in case of FRACOF model. The same type of insulation as for FRACOF model was considered for the edge beams, characterized by: 128 kg/m^3 specific mass, 0 kg/m^3 water content and a temperature dependent thermal conductivity from 0.04 W/mK at 20°C, to 0.48 W/mK at 1200°C. The variation of the thermal conductivity, thermal elongation and specific heat of steel function of temperature was considered as given in EN

1993-1-2 (2005). Other parameters considered for steel are: 7850 kg/m^3 specific mass and 0.7 surface emissivity. A siliceous type of concrete was considered. The upper limit of the thermal conductivity, according to EN 1992-1-2 (2005) was considered for concrete. Other parameters considered for the concrete within the composite slab are: 2400 kg/m^3 specific mass, 46 kg/m^3 water content and 0.7 surface emissivity. Due to the ISO fire exposure, for all materials, the convection coefficient on heated surfaces was considered 25 W/m^{2}K, while the convection coefficient on unheated surfaces was 9 W/m^{2}K.

The FE simulation was carried out for 180 min, even if the experimental program lasted for 123 min, in order to define the failure of the composite assembly.

For the thermal distribution, as in case of the FRACOF numerical model, the cross section of the slab containing ribs has been replaced by a section with an equivalent thickness calculated according to EN1994-1-2 Annex D (EN1994-1-2, 2005).

The primary and secondary beams have been idealized with beam elements and the slab with shell elements of uniform thickness. The beam-to-column and beam-to-beam connections have been modelled as pinned. The rebars have been idealized as a steel layer in amount of 251 mm²/m.

In the simulation, the load was considered uniformly distributed. For the material properties, the nominal values were considered.

In Figure 2.6, the calculated deformed shape and the membrane forces of the slab after 149 minutes are shown. At this moment the composite slab failed, in the same manner as for the model of FRACOF structure, due to the large deflections of the secondary edge beam. In the chart, a comparison between the measured and the calculated deflection in the center of the slab is shown.

After about 60 minutes a difference can be observed between the measured and the calculated deflection curves. In the test, for one of the secondary edge beams, damage of the insulation was observed, which was confirmed by an increase in temperature near the upper flange. For the mentioned edge beam, the measurements also show an increase of deflection at the middle of the span (see Fig. 3.9), affecting in this way the deflection in the middle of the slab. This effect, which could not be predicted before the test, has not been incorporated in the simulation.

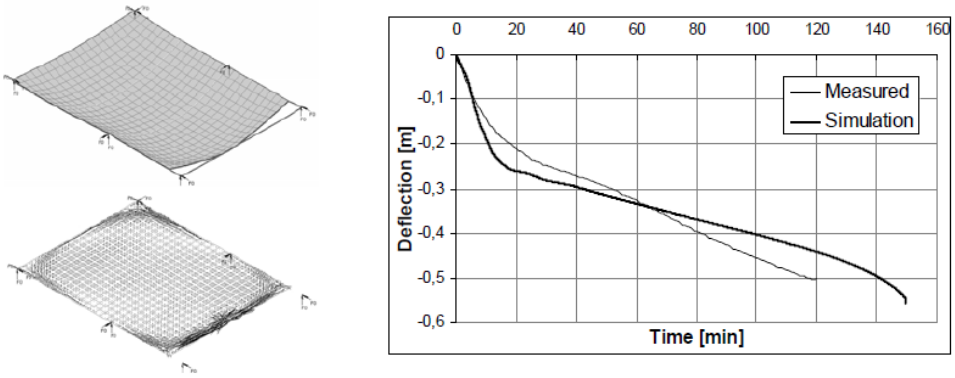

Fig. 2.6. Deformed shape and membrane forces – Deflection in the middle of the slab (Zaharia et al, 2013)

2.3. CONCLUSIONS MADE AFTER PREVIOUS FRACOF AND COSSFIRE TEST SIMULATIONS WITH SAFIR

The primary and secondary beams may been idealized using beam elements, and the slab using shell elements.

In order to obtain a simple numerical model, the cross section of the slab containing ribs may been replaced by a section with an equivalent thickness calculated according to EN1994-1-2. Annex D (2005).

An important option when the numerical model is built, is to consider or not the vertical restraints along the edge of the composite floor. For the FRACOF and COSSFIRE specimens, the failure highlighted by the numerical analysis was caused by plastic hinges forming in the secondary edge beams. When the edges of the slabs are completely restrained vertically, the plastic hinges forming in the secondary edge beams are avoided and the fire resistance times are significantly increased for these two slabs. Considering the results of the numerical simulations for these cases, it was recommended to avoid the vertical restraints on the edge of the composite floor, even if this would simplify the numerical model.

CHAPTER 3. FICEB TEST

The details of the fire test conducted at the University of Ulster within FICEB-RFCS Research Grants (see Figure 3.1-4), presented further in this chapter, are described in (MACS+, RFCS, 2014), (Vasart and Zhao, ECCS, 2013), (FICEB, RFCS, 2012). The choice of such compartment is more practical as it could be located near the central zone of any office building and able to cover an area of around 15 by 9m with an internal floor of 3.0m. The surrounding walls of the compartment were constructed using large blocks such as Ytong, except the facade where three openings considered concrete blocks were used. The surrounding walls were not fixed to the composite floor at the top and allow the vertical movement of the floor to have a realistic catenary action forces. All the columns were protected with plasterboards and the surrounding edge beams protect by spray systems that allows duration of fire resistance for around two hours.

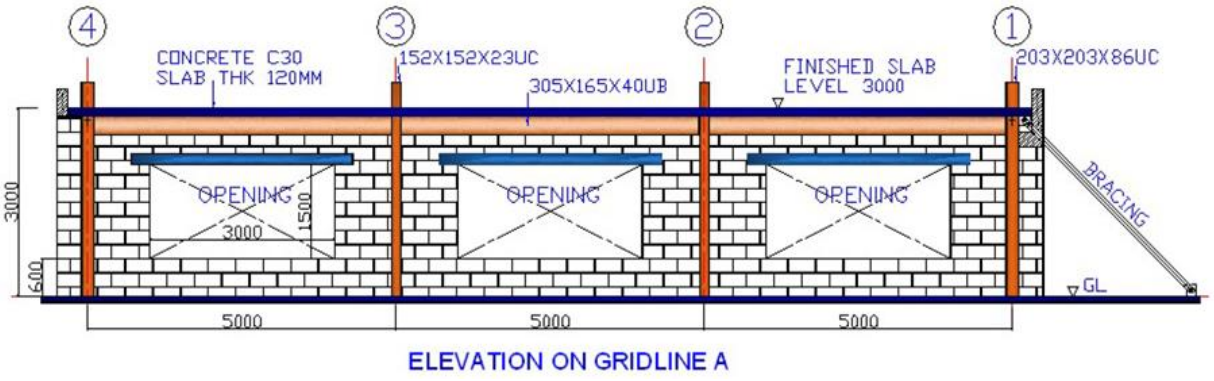

Fig. 3.1. Facade of the tested compartment (FICEB, RFCS, 2012)

Fig. 3.2. Compartment on fire (FICEB, RFCS, 2012)

The imposed load was simulated using sandbags each weight 10kN applied over an area of 15m by 9m. The ventilation area will consist of a single opening of 3.0m in length with 1.5m high situated at 0.6m from the level floor. The fire design parameters were calculated according to the EN 1991-1-2 (2005).

The two central secondary beams were unprotected. This test provided unique experimental data on the performance of the cellular beams acting in membrane action. The information recorded during the test was used to validate the natural fire safety concept and provide design rules and guidance for protected and unprotected cellular beams.

Fig. 3.3. Real structure of the test (inside view) (FICEB, RFCS, 2012)

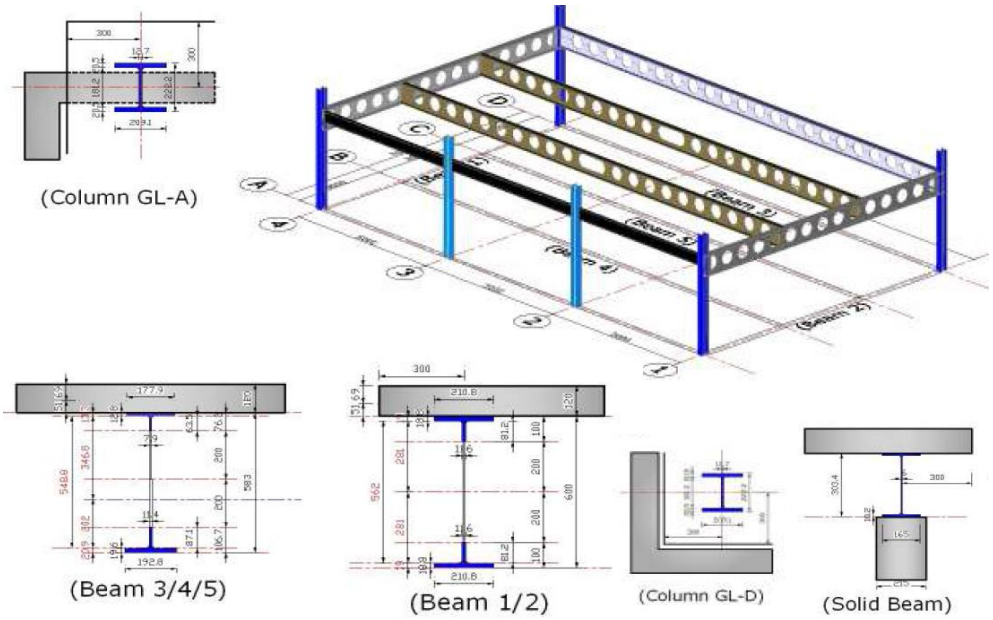

Fig. 3.4. 3D structure of the test with elements (MACS+, RFCS, 2014)

The front facade, with openings, was constructed such that the wall was extended up to the underside of the solid beam along gridline A, allowing no vertical deflection of the beam along this gridline. The frame was braced in the horizontal direction at the following locations; Column A1 was braced in both lateral directions, Column A4 was braced laterally parallel to gridline 4 and Column D1 was braced laterally parallel to gridline D. Bracing was provided using a diagonal CHS.

All the columns, and the solid beam along gridline A, were protected using commercially available 20mm thick fire board with a standard fire resistance period of 2 hours. The perimeter CBs on gridlines 1, 4, and D were protected using a ceramic fibre (see Fig. 3.5), which also provided a standard fire resistance period of 2 hours. The fire protection was fitted using an approved contractor, following the manufacturer's specification. Plasterboard, 15mm thick, was also used to cover the inner face of the boundary walls to reduce heat loss through the blockwork (Fig. 3.5).

Fig. 3.5. Fibre and plasterboard protection used inside the compartment (MACS+, RFCS, 2014)

The concrete composite slab was 120mm thick and comprised a 51mm deep, 1mm thick, Holorib steel deck (HR51/150), normal-weight concrete and mesh steel reinforcement. The dovetail steel deck had a measured tensile strength of 327N/mm^2. The welded wire A393 mesh reinforcement (Fig. 3.6) comprised 10mm diameter ribbed bars at 200mm centers, with nominal yield strength of 500N/mm^2, which was specified using the Bailey Method (Bailey, 2001 and 2004), based on the design parametric fire curve. The mesh reinforcement had a minimum lap length of 400mm and covered with 40mm thickness of concrete. The concrete mix design (for 1m^3) comprised: 320kg OPC, 918kg 10mm limestone, 691kg sharp sand, 380kg 6mm limestone, 30kg grey (recycled) water and 142kg cold (tap) water. No additives or air-entraining agent was used in the concrete mixture.

The measured average concrete compressive cubic strength was 50N/mm^2 on the day of test.

Full interaction between the slab and beams was achieved using shear connectors, of 19mm diameter and 95mm height, placed at 200mm centers along the beams. The requirement for U-bar reinforcement around the slab's perimeter (as shown in Fig. 3.6) is not a special requirement for fire design, but was needed to ensure correct reinforcement detailing for ambient design. The U-bars were 10mm diameter and placed with 30mm cover to the edge of the slab, as shown in Fig. 3.6.

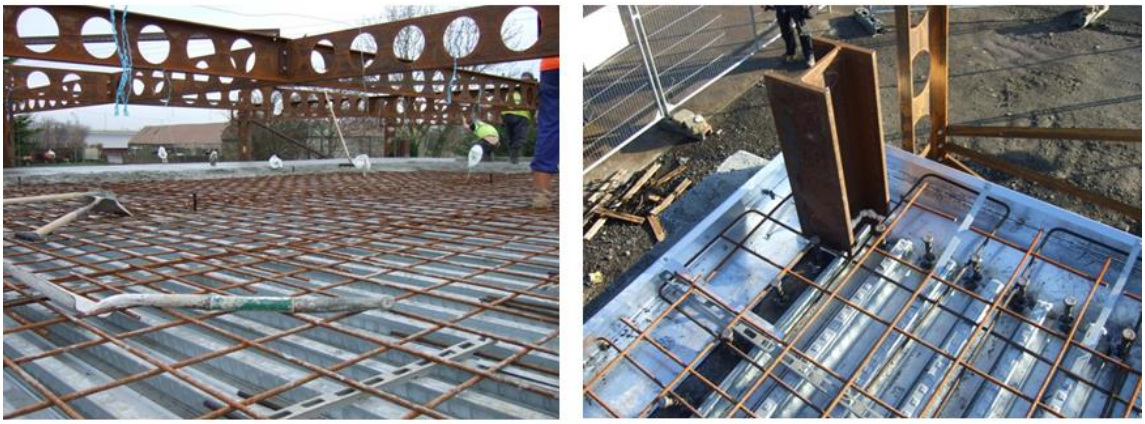

Fig. 3.6. Mesh reinforcement and steel decking before concrete casting (MACS+, RFCS, 2014)

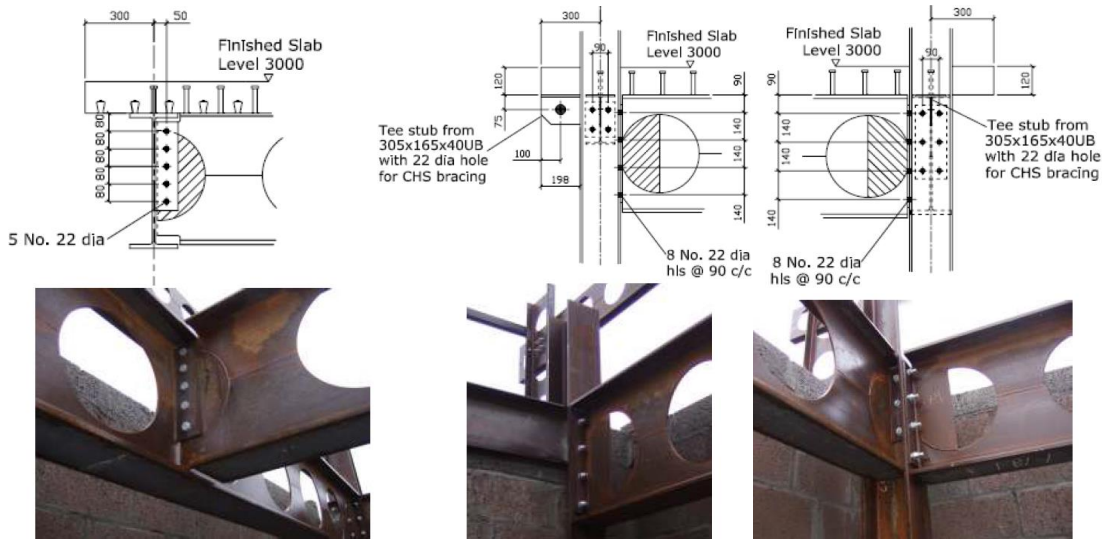

Fig. 3.7. Beam-beam and beam-column connections (MACS+, RFCS, 2014)

The loads used within the structure are the same as those which are commonly used in the design of office buildings and are as outlined in Table 3.1.

description	Characteristics KN/m^2	Fire Factor	Design Load KN/m^2
Partition	1.0	1.0	1.0
Services & Finishes	0.5	1.0	0.5
Live Load	3.5	0.5	1.75
		Total	3.25

Table 3.1. Design loads (FICEB, RFCS, 2012)

The applied load of 3.25 kN/m² will be achieved using 42 sandbags (each weighting 1t) evenly positioned over the floor plate, as shown in Fig. 3.8. The floor plate is 9 by 15m; this gives an applied load of 3.25 kN/m². The self-weight of the slab of 120 mm thickness is about 2.90 kN/m², creating a total load of 6.15 kN/m².

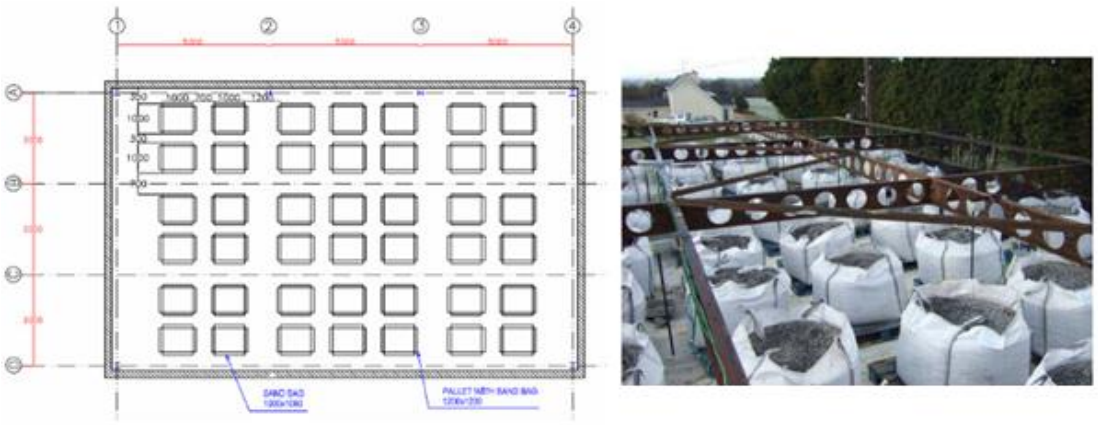

Fig. 3.8. Vertical static load with the plan view (FICEB, RFCS, 2012)

Assuming the design for an office, the fire load density would be 511 MJ/m2 according to Table E.2 of EN 1991-1-2 (2005). However, for this test, the fire load was increased by using 45 standard (1 m x 1 m x 0.5 m high) wood cribs, comprising 50 mm x 50 mm x 1000 mm wooden battens, positioned evenly around the compartment (Fig. 3.9), yielding a fire load was 40 kg of wood per

square metre of ground area. The wood density provided was 510 kg/m^3 with a calorific value of 17.5 MJ/kg for wood, which corresponds finally to a fire load of 700 MJ/m^2. This is consistent for multi-storey office accommodation and allows a direct comparison with previous test carried out on the steel building at Cardington. The figure is well established from the statistical data and a number of tests have been carried out considering the quantity of fire load as the variable parameter.

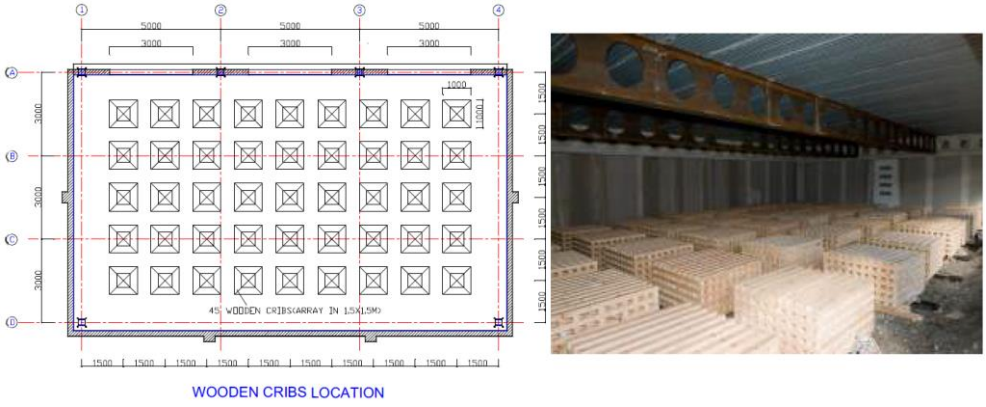

Fig. 3.9. Wooden cribs used for the fire load with the plan view (FICEB, RFCS, 2012)

The fire was started from a single ignition source (see Fig. 3.10). After 5 minutes two additional ignitions sources were started in different places and the rest of cribs were left to ignite naturally (see Fig. 3.11).

Each crib was connected to its neighbours by mild steel channel section with porous fibre board laid into the channels and, approximately 30 minutes before ignition, some 20 litres of paraffin was poured into channel.

The ambient temperature prior to the test was 5°C. The maximum recorded atmosphere temperature in the centre of the compartment was 1053°C around 500 mm from the ceiling after 75 minutes.

Under fire conditions, the deflection in the steel beam is the result of two causes: the thermal bowing and the mechanical deflection. The mechanical

deflection is the increase in deflection under constant load due to reduced steel strength and stiffness with increasing temperatures. At higher temperatures, mechanical deflection dominates and the beam deflection increases at a faster rate with a rise in the beam temperature. **The unprotected cellular beams became as cables with only top flange considered working at very temperature around 800°C.** Therefore, the bottom flange became very weak; the vertical shear forces induced by each web post combined with longitudinal restraint provided by the concrete slab caused a rotation of the lower beam.

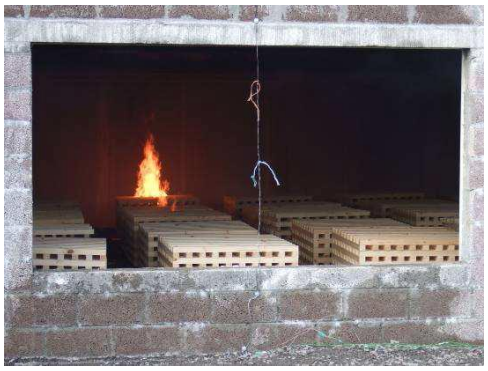

Fig. 3.10. Fire ignition (MACS+, RFCS, 2014)

Fig. 3.11. Fully engulfed fire (MACS+, RFCS, 2014)

The main requirements of the instrumentation are to measure the temperature, the deflected shape of the floor and the main structural elements. The instrumentation includes thermocouples and displacement transducers.

Around 300 thermocouples were used to monitor the temperature in the beams (protected and not protected) within the compartment the temperature distribution through the slab and the atmosphere temperature within the compartment (see Fig. 3.12).

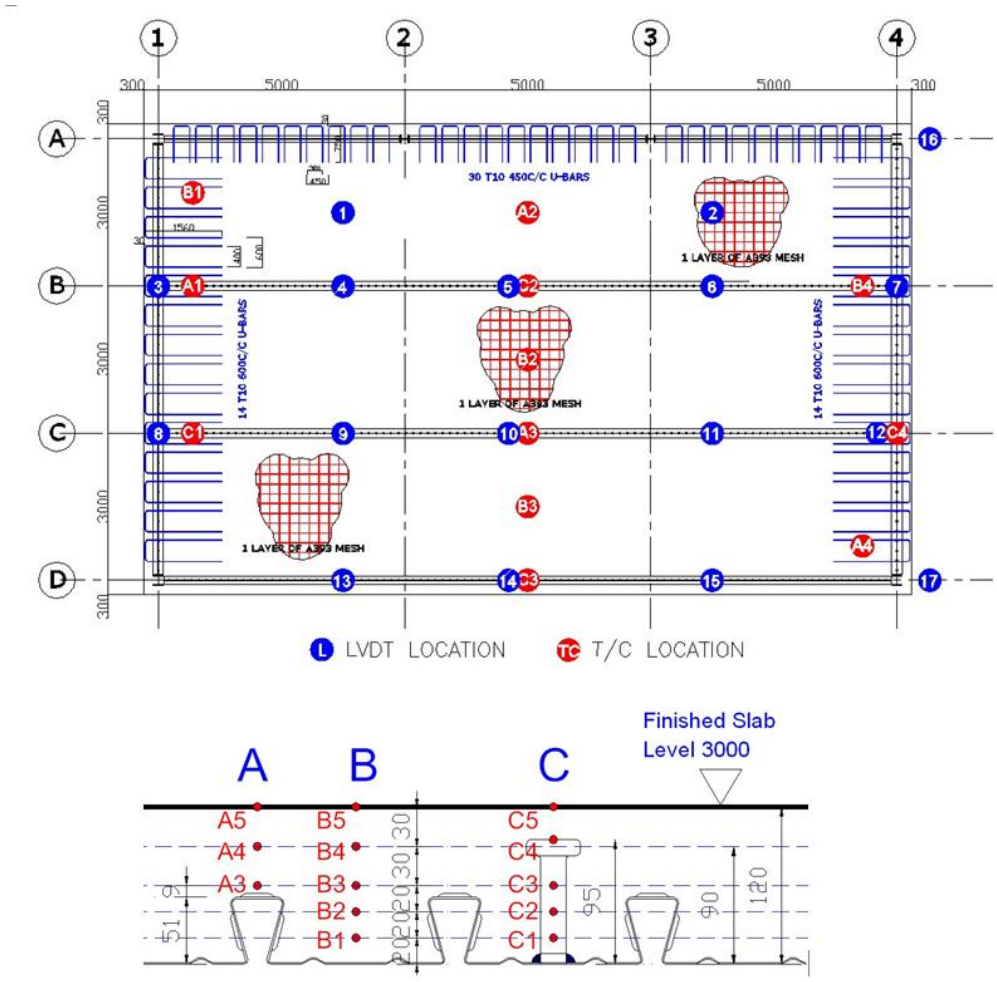

Fig. 3.12. Location of thermocouples in the test (MACS+, RFCS, 2014)

CHAPTER 4. NUMERICAL SIMULATION

4.1 SAFIR SOFTWARE

All the numerical simulations done for this work, were made with SAFIR (Franssen, 2005 and 2007), a special purpose computer program, developed for the analysis of structures under ambient and elevated temperature conditions. The program, which is based on the Finite Element Method (FEM), can be used to study the behavior of one, two and three-dimensional structures.

As a finite element program, SAFIR accommodates various elements for different idealization, calculation procedures and various material models for incorporating stress-strain behavior. The elements include the 2-D SOLID elements, 3-D SOLID elements, BEAM elements, SHELL elements and TRUSS elements. The stress-strain material laws are generally linear-elliptic for steel and non-linear for concrete.

For any analysis using SAFIR, data files acting as input files to the program are prepared. For each analysis type (thermal, torsional or structural analysis), the user prepares one data file. This is an ASCII file, created with a text editor, in a word processor, or by SafirWizard (for special cases only), and it must have the file type .IN.

This file with a .IN extension contains information such as calculation strategy, time discretization, loads, node coordinates, types of finite elements used, material properties, etc.

For structural analysis, the .IN file specifies the name of the .TEM files created during thermal and torsional analyses and in which the temperature data is stored. Fig. 4.1.1 shows a schematic representation of the different steps and files that may be involved in the case of a frame structure comprised of two types

of different sections, one for the columns and one for the beam. The user must create the .IN files.

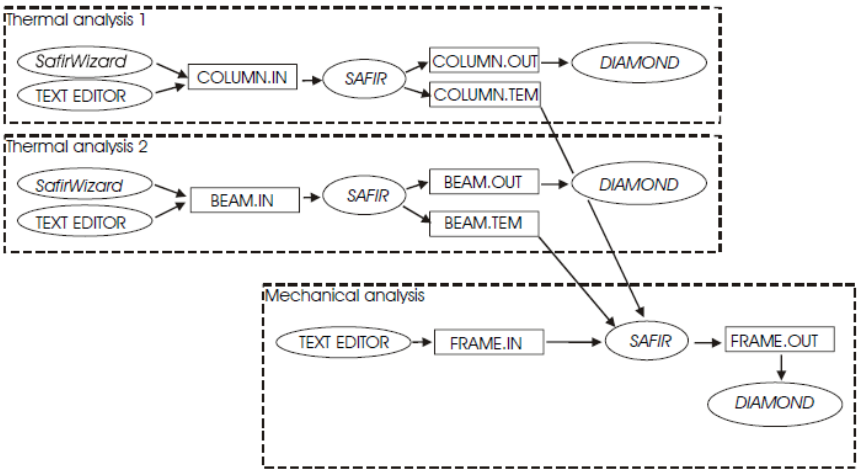

Fig. 4.1.1. Files and steps (Franssen 2007)

For all the simulations of the test, 3D analysis were done, in which beam elements for the protected primary beams and for the unprotected secondary beams were placed in the middle area of the slab. For the modelling of the composite slab, shell elements were used. Descriptions and assumptions of these type of elements presented below.

A - The BEAM Elements

The beam element (see Fig. 4.1.2) is straight in its un-deformed geometry. Its position in space is defined by the position of three nodes: the two end nodes (N1-N2), and a third node (N4) defining the position of the local y axis of the beam. The node N3 is used to support an additional degree of freedom.

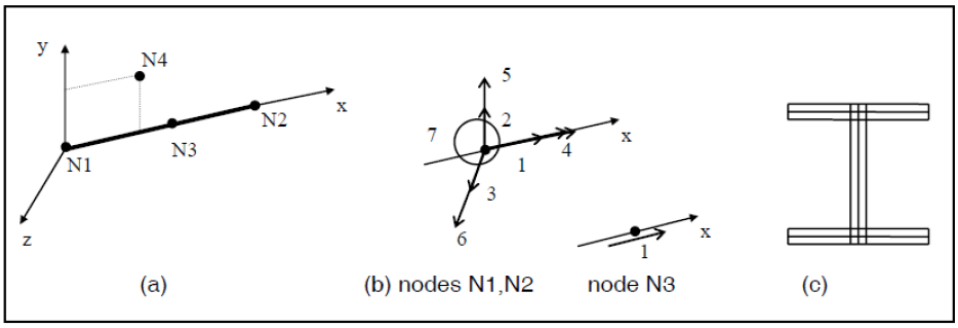

Fig. 4.1.2. Beam element: (a) Local axes (b) Degrees of freedom at nodes (c) Cross section (Franssen 2007)

To describe the geometry of the cross section, the fiber model is used. The cross-section of the beam subdivided into small fibers (triangles, quadrilaterals or both). The material behavior of each fiber is calculated at the center of the fiber and it is constant for the whole fiber. Each fiber has its own material, this allows for the building of composite sections made of different materials.

Assumptions for beam elements:

• the Bernoulli hypothesis is considered, i.e., the cross section remains plane under bending moment;

• plasticization is only considered in the longitudinal direction of the member, that is uniaxial constitutive models;

• non-uniform torsion is considered.

B - The SHELL Element

B.1 Geometry

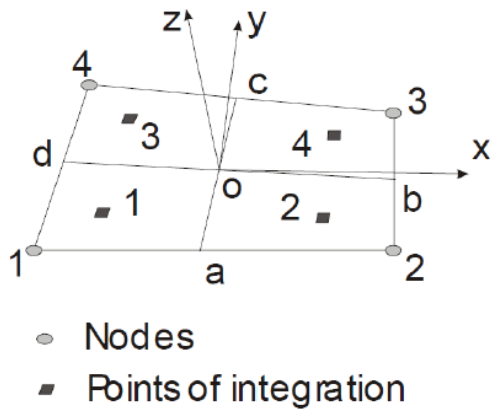

Fig. 4.1.3. Definition of the geometry and local axes (Franssen 2007)

The nodes are in the order 1, 2, 3, 4; a, b, c, d are the middle points of the edges of the elements (see Fig. 4.1.3). o, the centre of the local system of co-ordinates is at the intersection between a-c and b-d; z has the direction of d-b ^ a-c; x and y are perpendicular to z and their direction is chosen as to have the same angle between o-b and x, on one hand, and o-c and y, on the other hand. As a particular case, if the element is a plane rectangle, x is the median 0-b and y is the median o-c.

B.2 Points of integration

There are four points of integration on the surface of the element, see Figure 4.1.3. In each direction, the integration is by the method of gauss. The number of integration points on the thickness is chosen by the user, from 2 to 10. The integration is also by the method of Gauss.

B.3 Rebars

Different layers of rebars can be present in the element. The rebar layers are horizontal (i.e. parallel to the local x, y plane). The rebars are uniformly distributed (layered rebars). Each layer is defined by:

• it's local vertical coordinate z in the element (this level must not necessarily coincide neither with the position of a point of integration on the thickness, nor with a position where the temperature has been calculated. Linear interpolations are made);

• it's cross section per unit length of width (m^2/m for example);

• it's material number;

• the angle between the direction of the rebars and the local x axis.

Assumptions for rebar elements are:

• the cross section of the rebar is not subtracted from the plane section of the element. This means that, in a reinforced concrete slab, steel and concrete are supposed to be simultaneously present at the location of the bars,

• the bars resist only axial direction actions. This means that a mesh of perpendicular rebars does not resist shear by itself.

Figure 4.1.4 is made for a rectangular element, and shows the way in which the angle is measured.

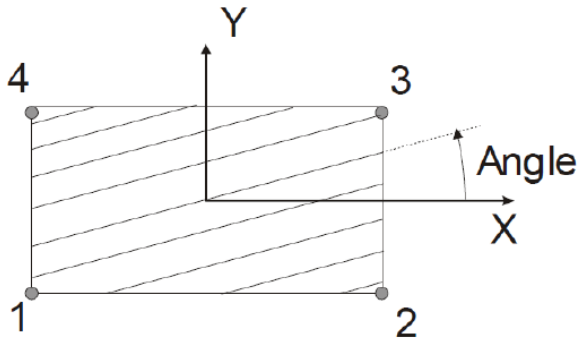

Fig. 4.1.4. Definition of the variable – angle (Franssen 2007)

4.2 PREVIOUS SAFIR SIMULATION OF FICEB TEST

In a previous attempt to model the behavior of the composite slab under natural fire (FICEB test), using SAFIR software, several assumptions were made by (MACS+, RFCS, 2014), (Vasart and Zhao, ECCS, 2013), (FICEB, RFCS, 2012), described in the following.

The fire was simulated with Ozone (see Fig. 4.2.1) instead of using real natural fire. The maximum temperature was 884°C after 60th minutes. The flashover occurs after 18th minute and the temperature remains higher than 500°C until the 91st minute.

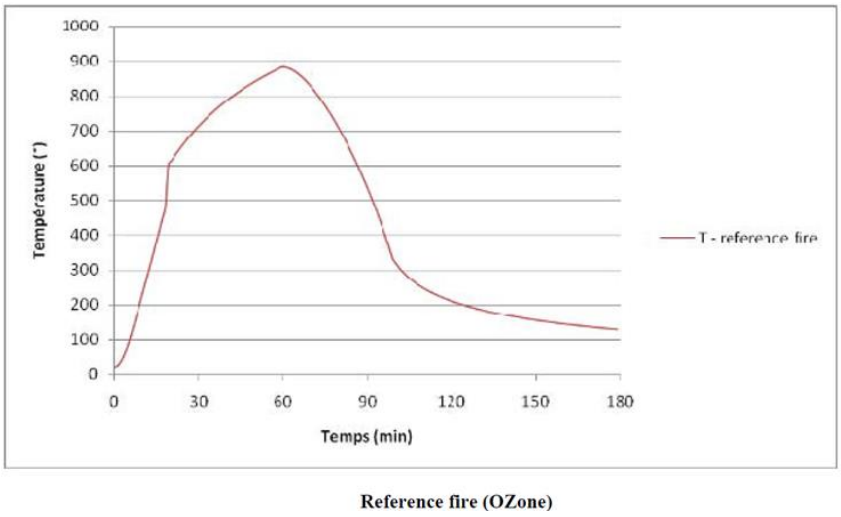

Fig. 4.2.1. Ozone fire curve (FICEB, RFCS, 2012)

In this simulation was used assumptions obtained from previous FRACOF and COSSFIRE simulations done by Zaharia et al., 2013. Such as:

- Primary and secondary beams have been idealized using BEAM elements, and the slab using SHELL elements;
- Instead of ribbed cross-section, equivalent thickness of the slab has been used according to EN1994-1-2. Annex D (2005);

Conservatively it was assumed that web post buckling would occur at temperature of 600 °C (see Fig.5.2.2).

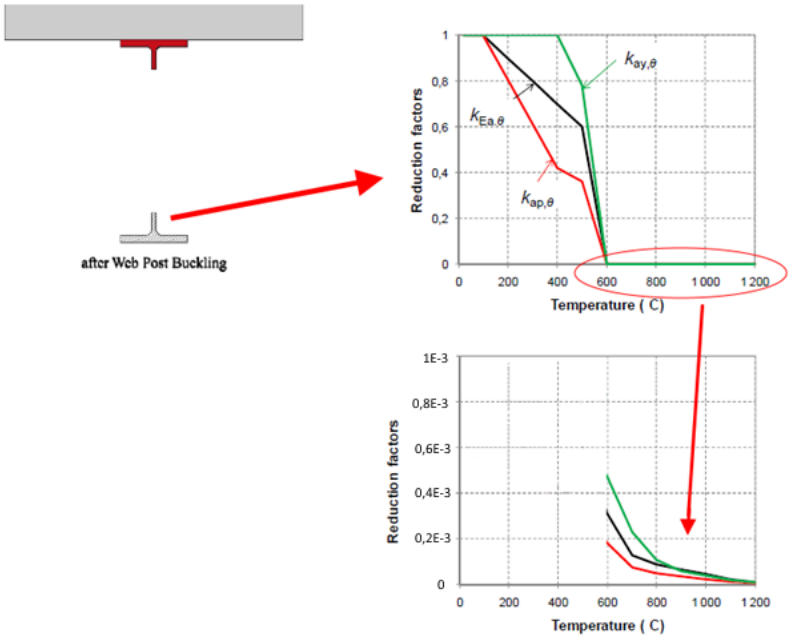

Fig. 4.2.2. Web post-buckling simulation (FICEB, RFCS, 2012)

Figure 4.2.3 shows the comparison between measured and computed vertical deflection at the middle of one of the unprotected cellular beams.

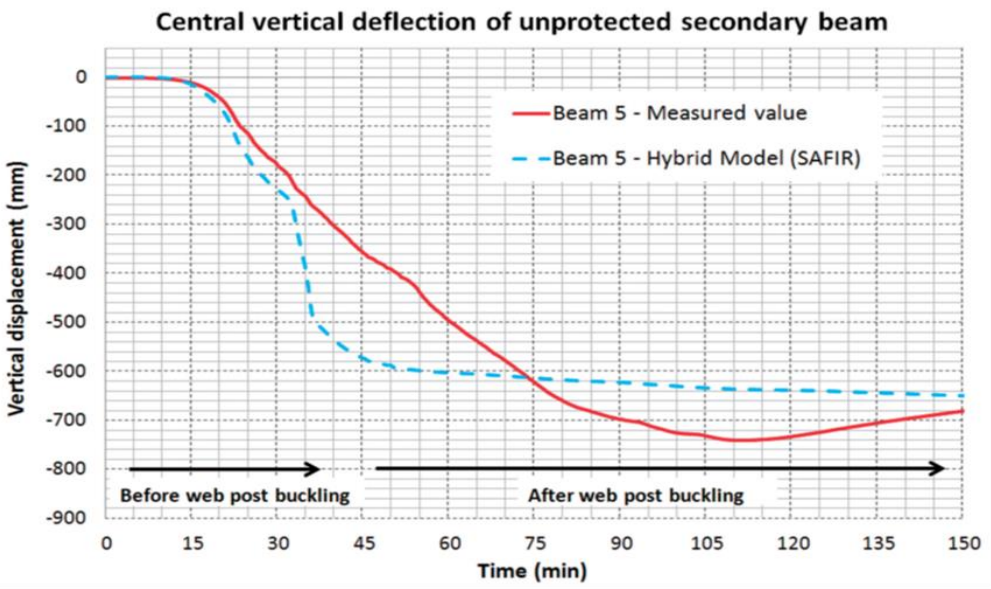

Fig. 4.2.3. Comparison between measured and computed vertical deflection at the middle of the unprotected beam (FICEB, RFCS, 2012)

4.3 NUMERICAL MODEL

4.3.1 FIRE LOAD

The first and the most important step, is to model the fire load for each member (instead of having a unique fire curve on the entire compartment). Experimental results regarding the evolution of the temperature in different points of the fire compartment are available (see Fig. 4.3.1.1) (FICEB, RFCS, 2012), so will be used in the numerical model.

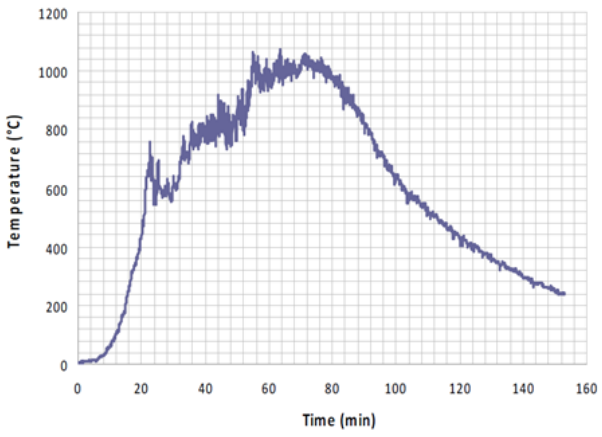

Compartment temperature at center

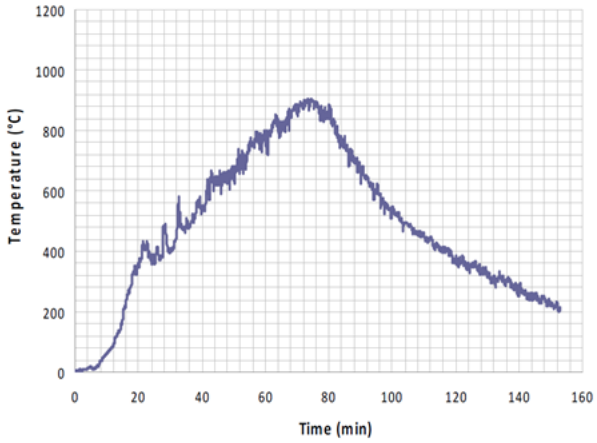

Compartment temperature at left back corner

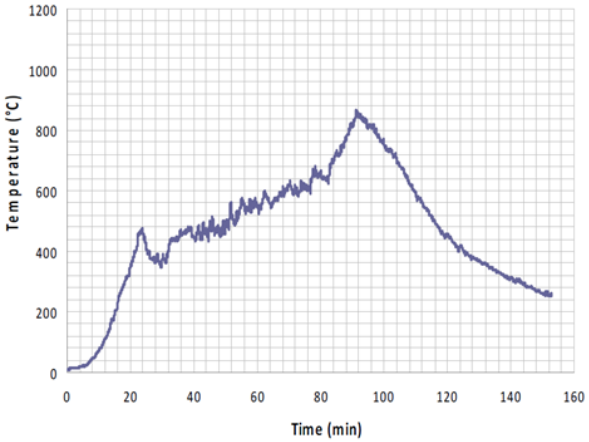

Compartment temperature at right back corner

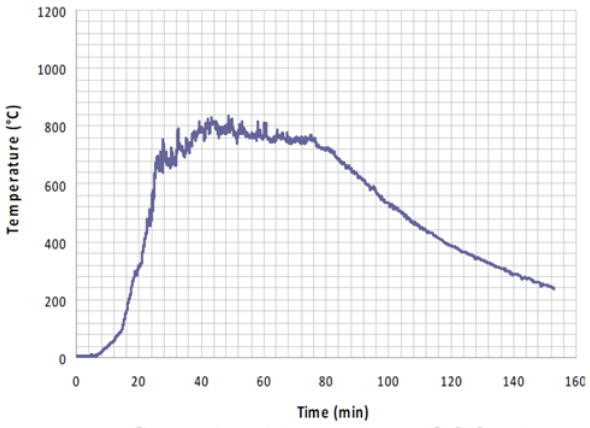

Compartment temperature at left front corner

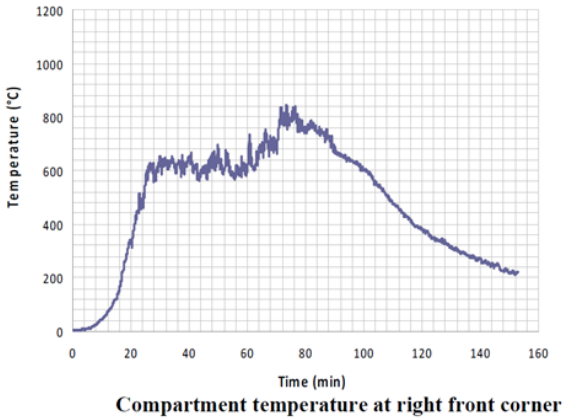

Fig. 4.3.1.1. Fire curves measured in different corners and the middle of compartment (FICEB, RFCS, 2012)

Several models have been tried with "exact" (see Fig. 4.3.1.2) and smoothed (see Fig. 4.3.1.3) fire load curve.

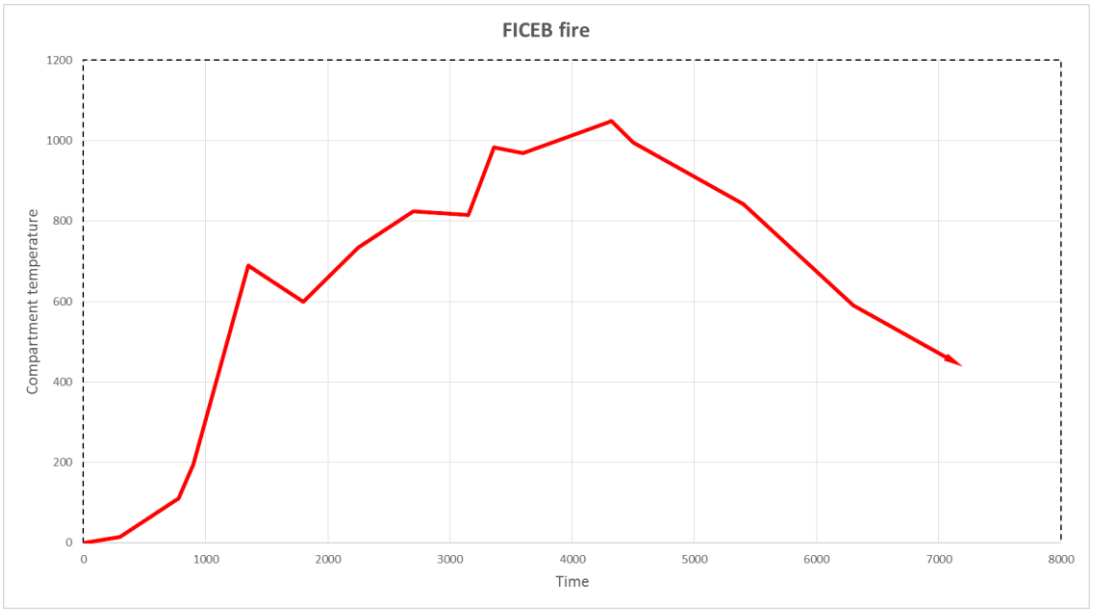

Fig. 4.3.1.2. "Exact" fire curve

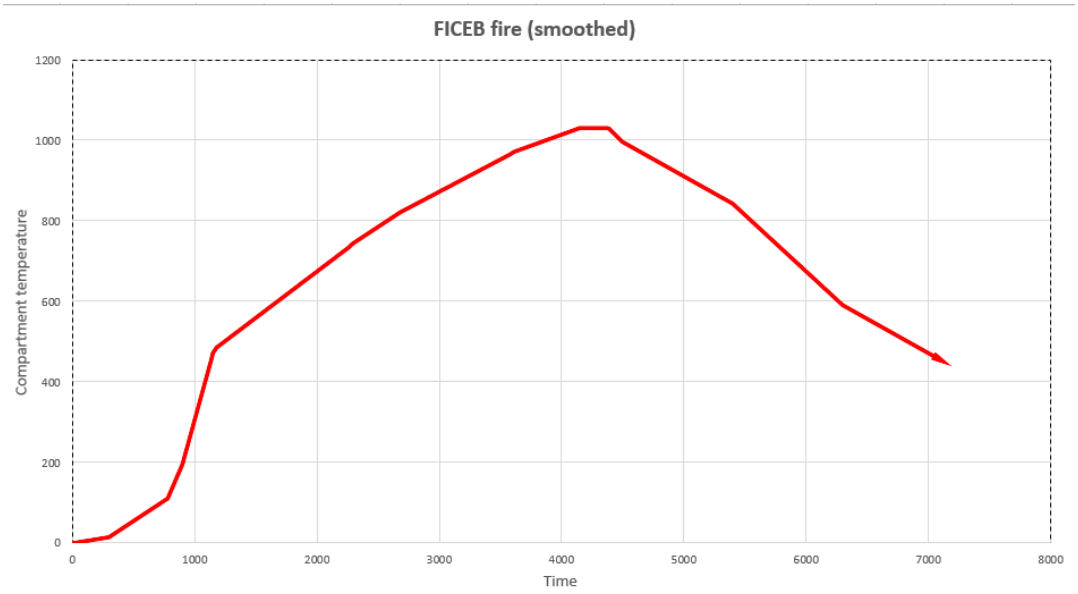

Fig. 4.3.1.3. Smoothed fire curve

Application of different temperatures (see Fig. 4.3.1.1) to different beams (see Fig. 4.3.1.4) were also used, but as only temperatures in the corners and in the middle of the compartment were known, it was necessary to overlap the corners fire load curves and applied the maximum values to the beams.

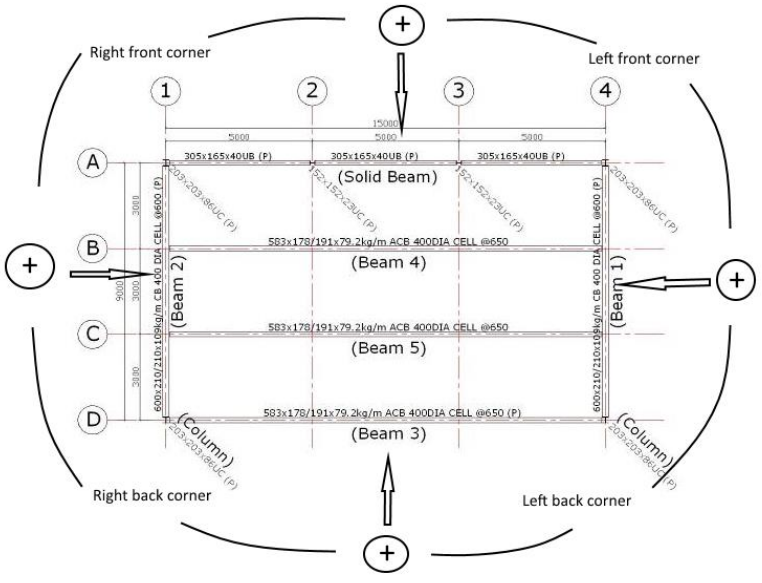

Fig. 4.3.1.4. Application of fire curves to beams (FICEB, RFCS, 2012)

Finally, fire curves shown in Figure 4.3.1.5 were used in the calculation.

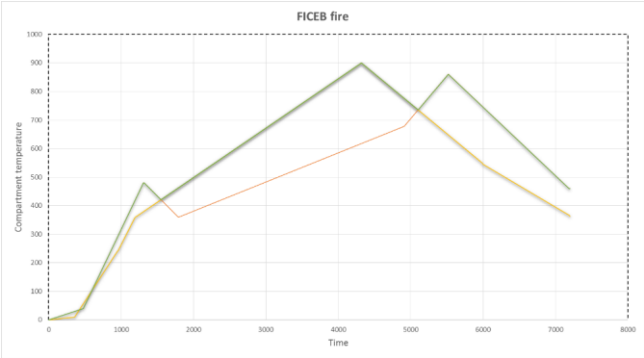

Right Back Corner +Left Back Corner

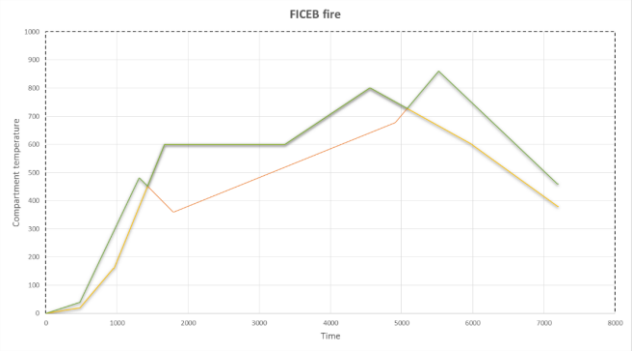

Right Back Corner + Right Front Corner

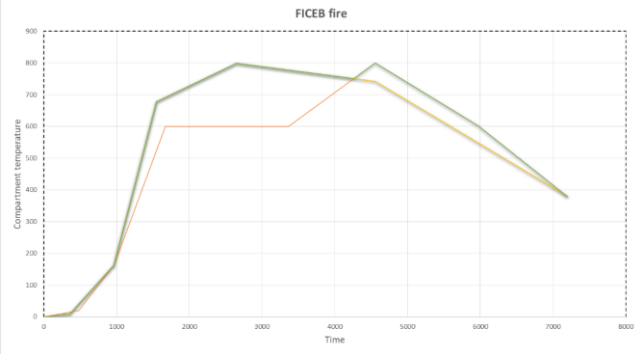

Right Front Corner + Left Front Corner

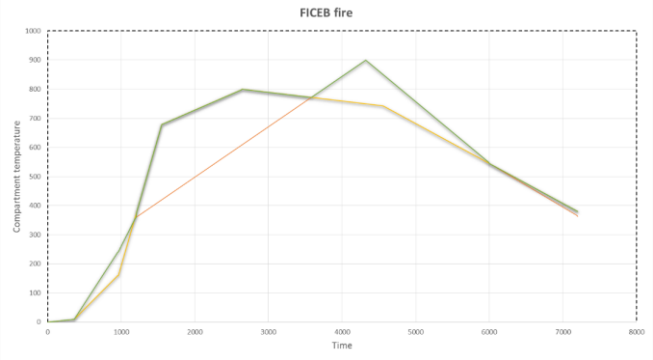

Left Back Corner + Left Front Corner

Fig. 4.3.1.5. Obtained fire curves for protected edge beams

4.3.2 CROSS-SECTIONS

The cross-section of each member was created independently and analyzed at elevated temperatures. In case of the cellular beam, the weakest cross-section (in the section of maximum radius of the cellular void of the web) was considered. Such assumption has shown good results and allowed the predicted behavior to be on the safe side. Figures 4.3.2.1-6 show the cross-sections models and the corresponding elements within the structure.

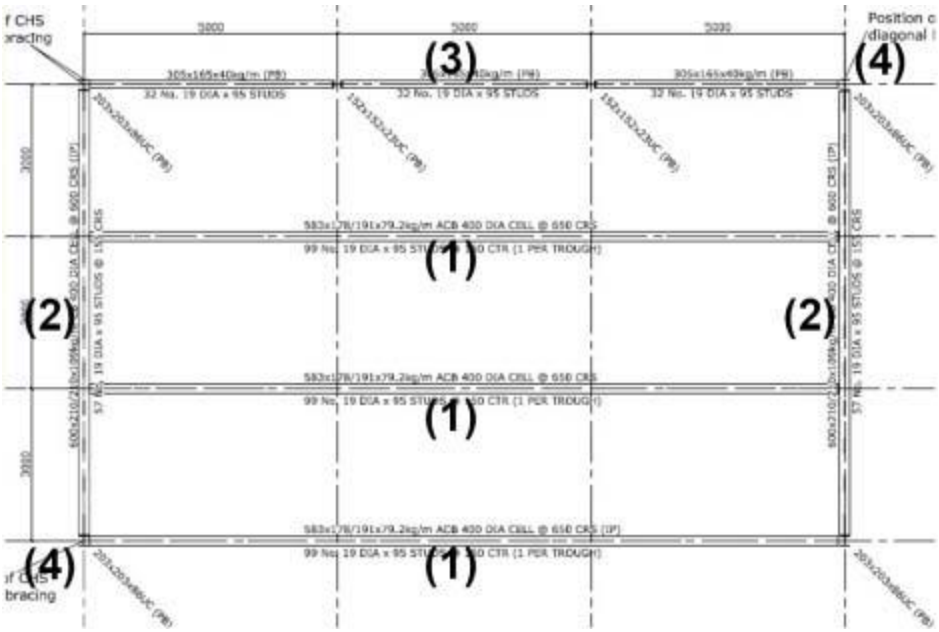

Fig. 4.3.2.1. Plan view of the compartment (FICEB, RFCS, 2012)

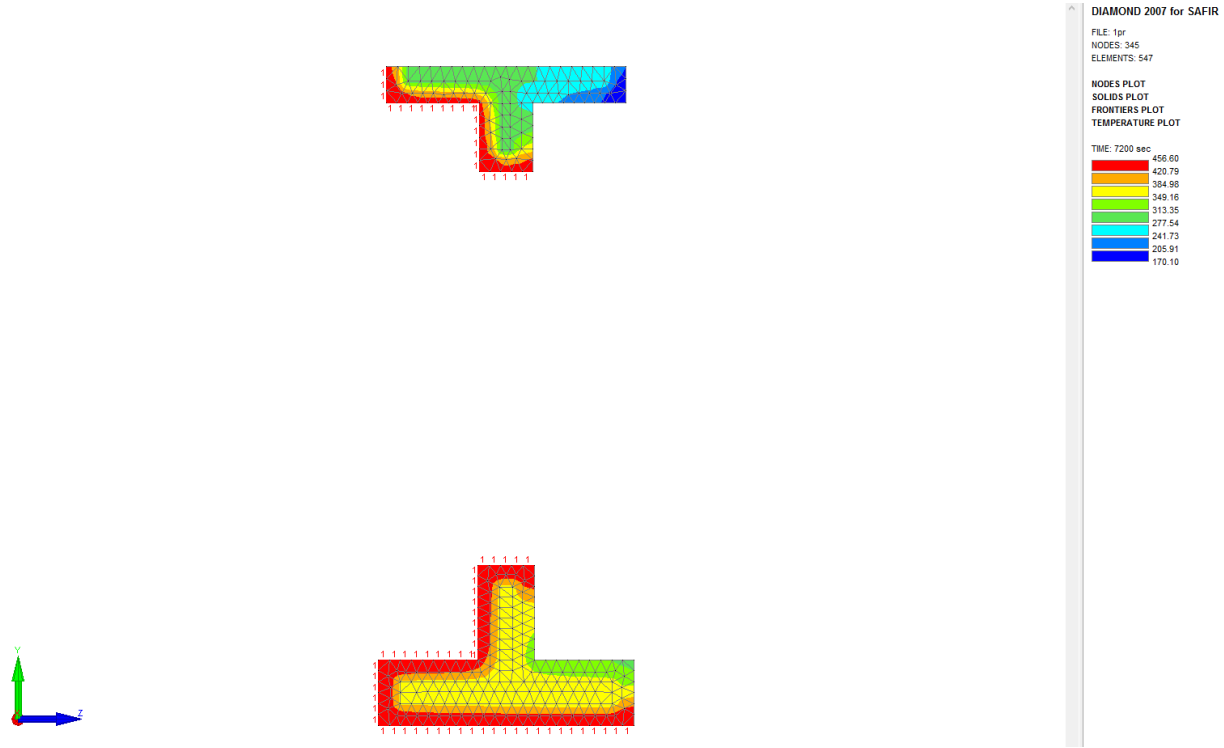

Fig. 4.3.2.2. Temperature distribution in cross section of protected edge cellular beam (1)

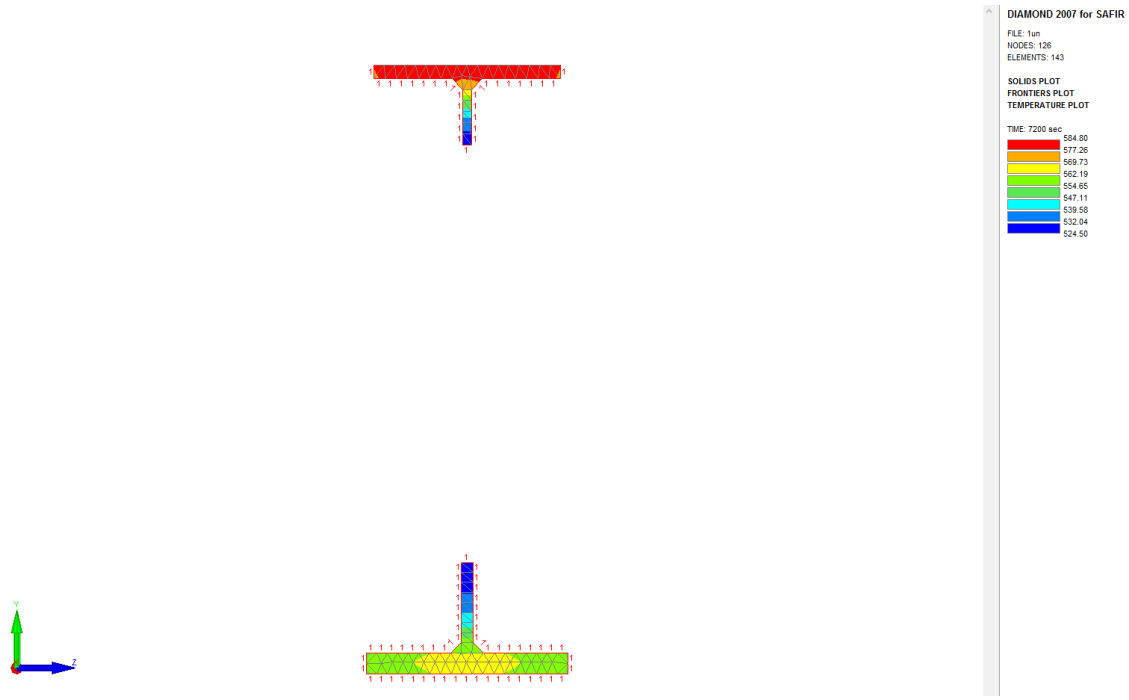

Fig. 4.3.2.3. Temperature distribution in cross section of unprotected secondary cellular beam (1)

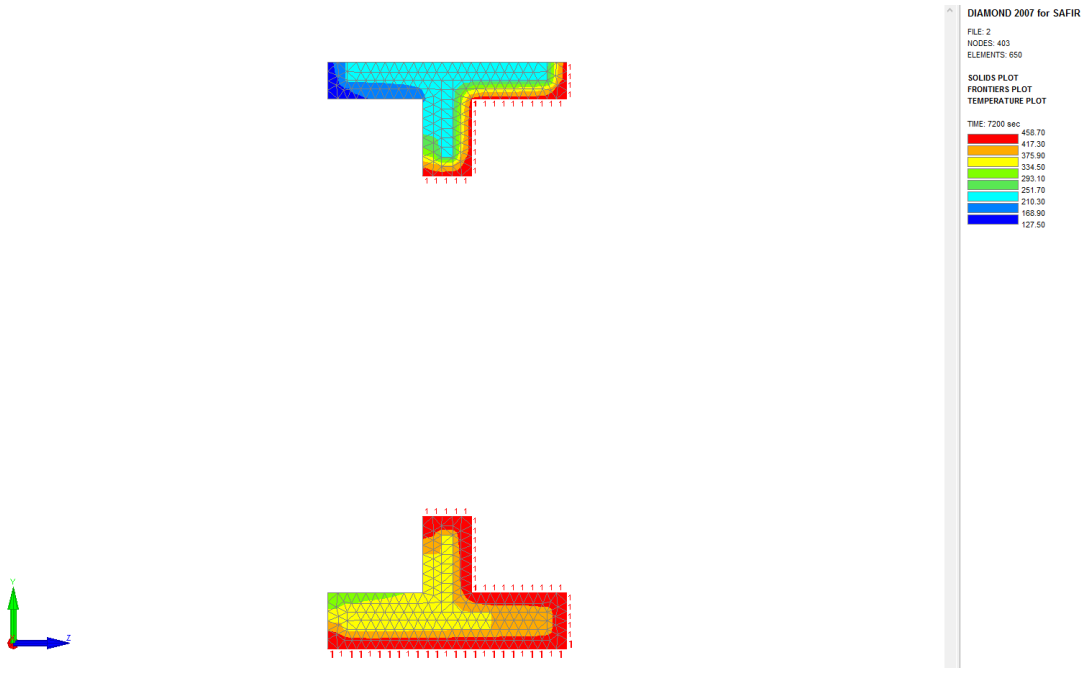

Fig. 4.3.2.4. Temperature distribution in cross section of protected edge cellular beam (2)

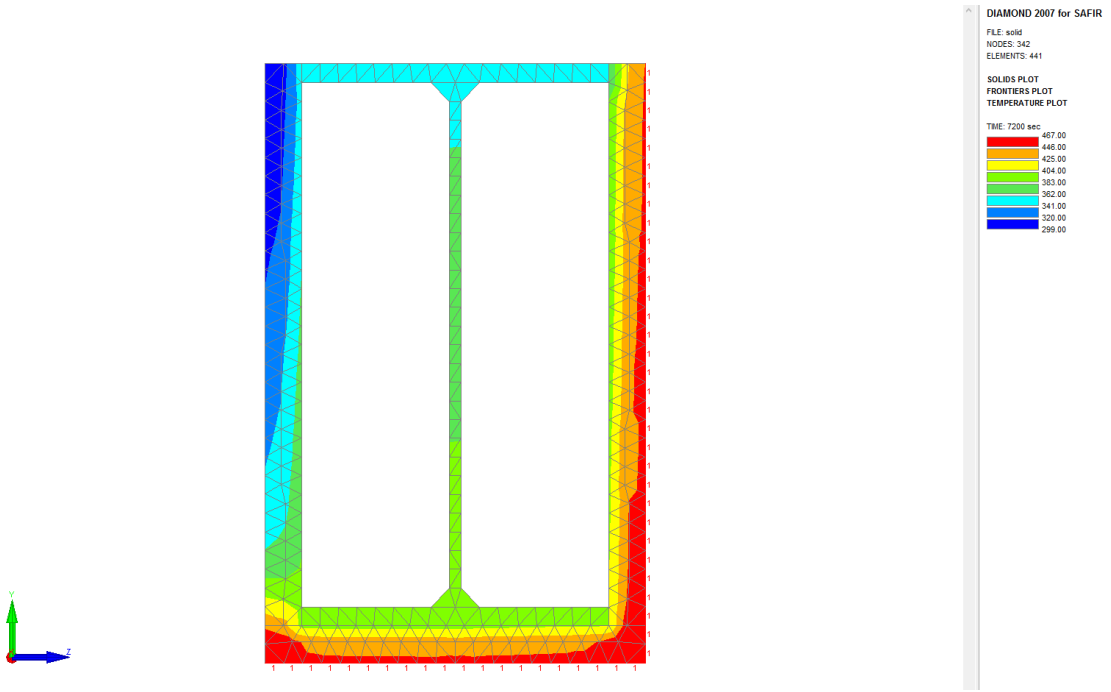

Fig. 4.3.2.5. Temperature distribution in cross section of protected edge solid beam (3)

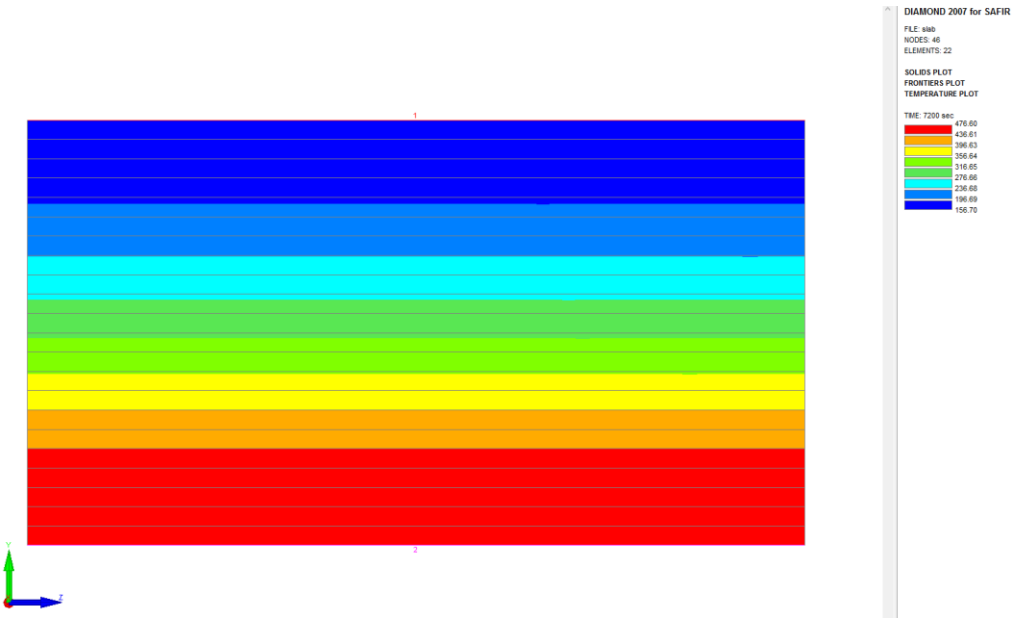

Fig. 4.3.2.6. Temperature distribution in cross section of the slab (using the equivalent thickness)

4.3.3 REINFORCEMENT LAYER

The third step is to introduce rebar mesh in the slab. The numerical model should consider the fact that the centre of the gravity of the slab will be in the middle of the effective thickness section, but the distance between the centre of the slab and the centre of the beam will be increased due to the thickness of the real composite slab thickness.

In its central part, the slab has a reinforcement mesh of 393 mm²/m in both directions. On a 2.4 m wide section on each side, the slab has a reinforcement mesh of 786 mm²/m in both directions (see Fig. 4.3.3.1). The T10 additional bars @200 on 2.4 m wide section each end of slab are centrally placed in the same layer with the mesh.

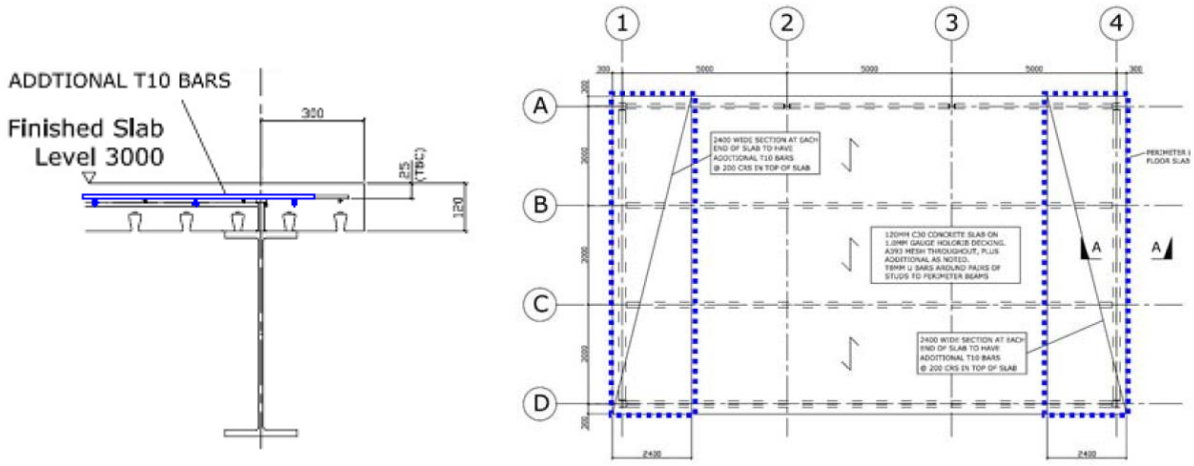

Fig. 4.3.3.1. Reinforcement mesh of the slab (FICEB, RFCS, 2012)

4.3.4 3D MODEL

Fig. 4.3.4.1 shows the considered structure containing just the beam elements, and Fig. 4.3.4.2 shows only the shell elements.

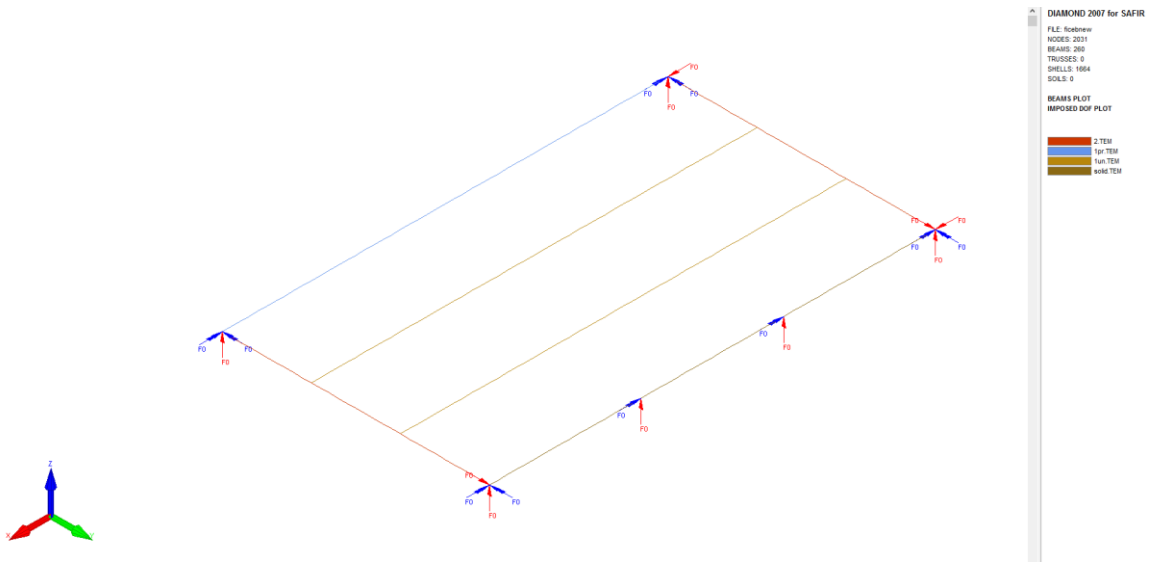

Fig. 4.3.4.1. Beam elements used for structural analysis.

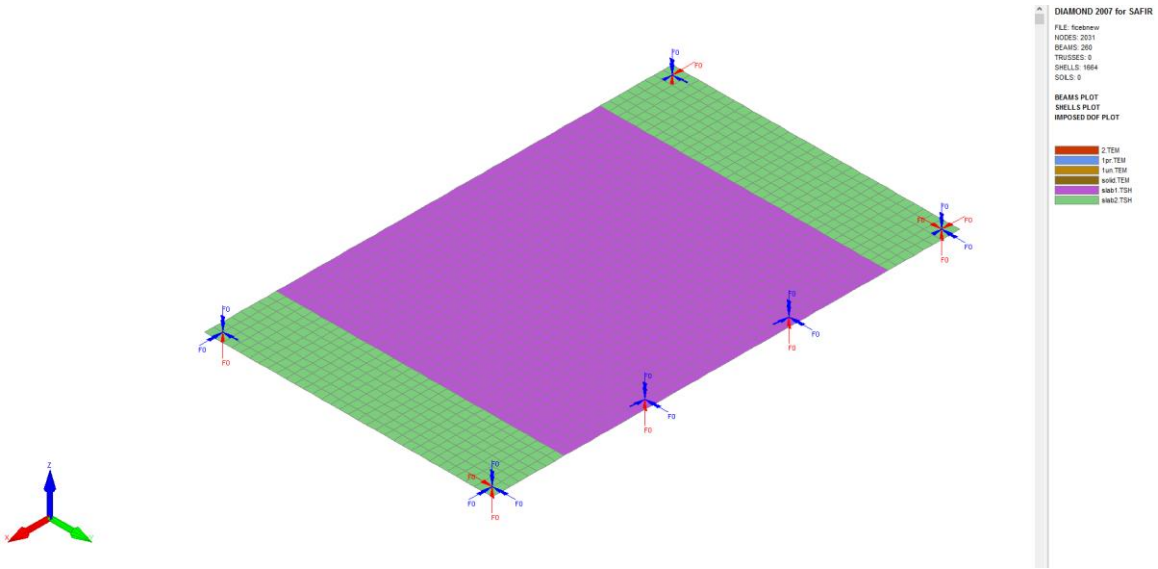

Fig. 4.3.4.2. Shell elements used for structural analysis.

The numerical simulations made for FRACOF test by Vulcu (2009) has showed that the model might be simplified by using appropriate supports (see Fig. 4.3.4.3) instead of adding column members in the model. This leaded to minor changes in the results but the calculation process takes less time.

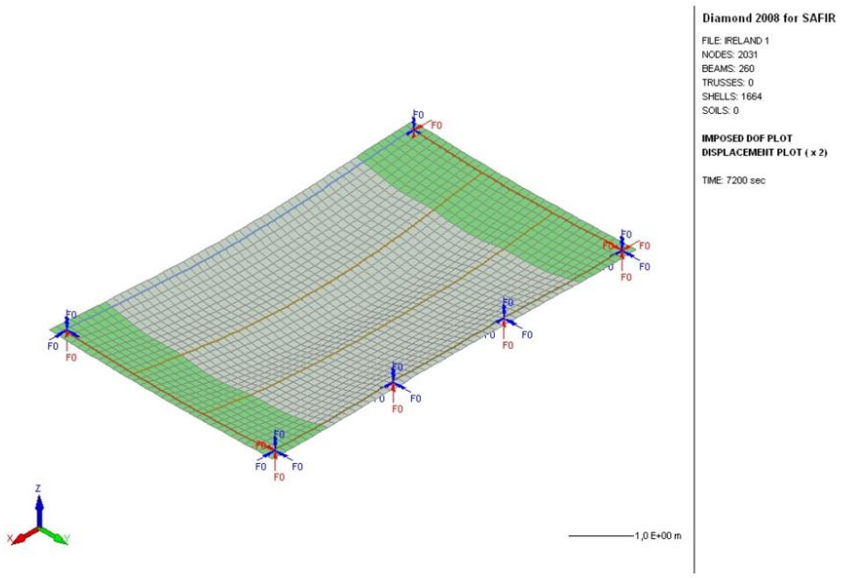

Fig. 4.3.4.3. Composite slab without columns

The loading was assumed as a distributed along the slab (see Fig. 4.3.4.5), instead of considering the precise location of each sand bag used in the tests (concentrated load was also studied). Figures 4.3.4.5-6 represents deflection and membrane action in the slab with the distributed loading.

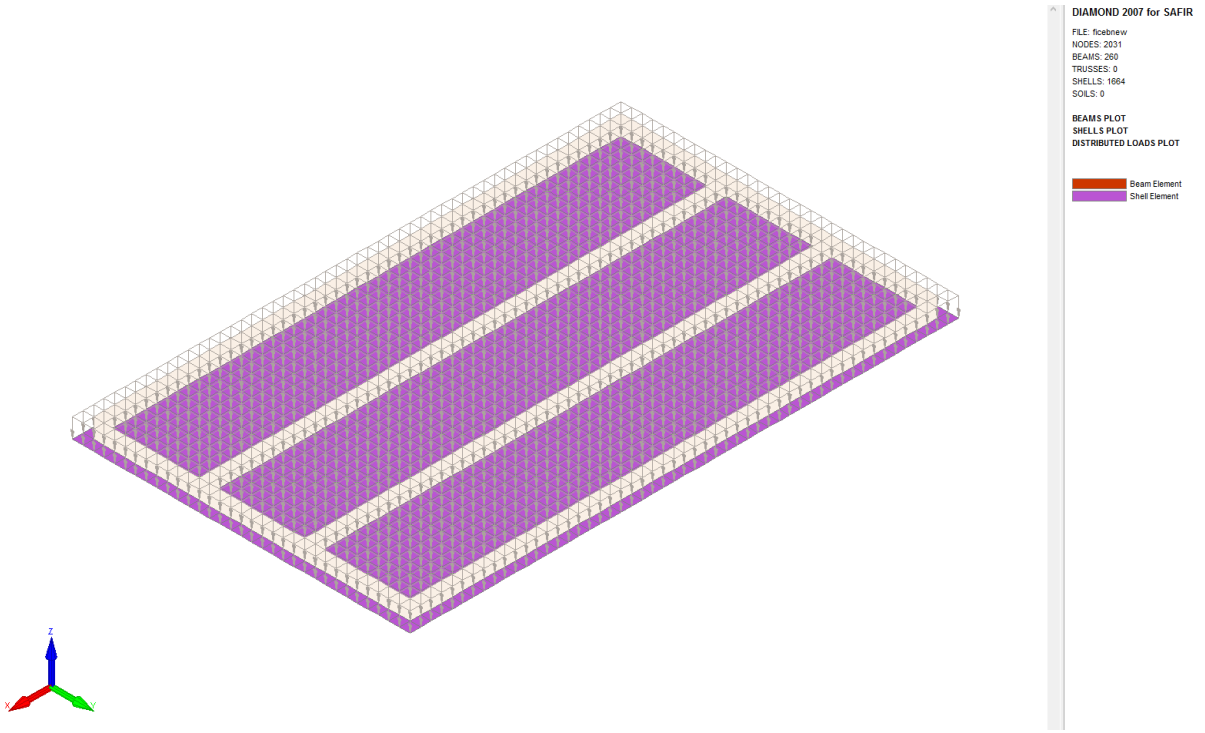

Fig. 4.3.4.4. Loading of the composite structure

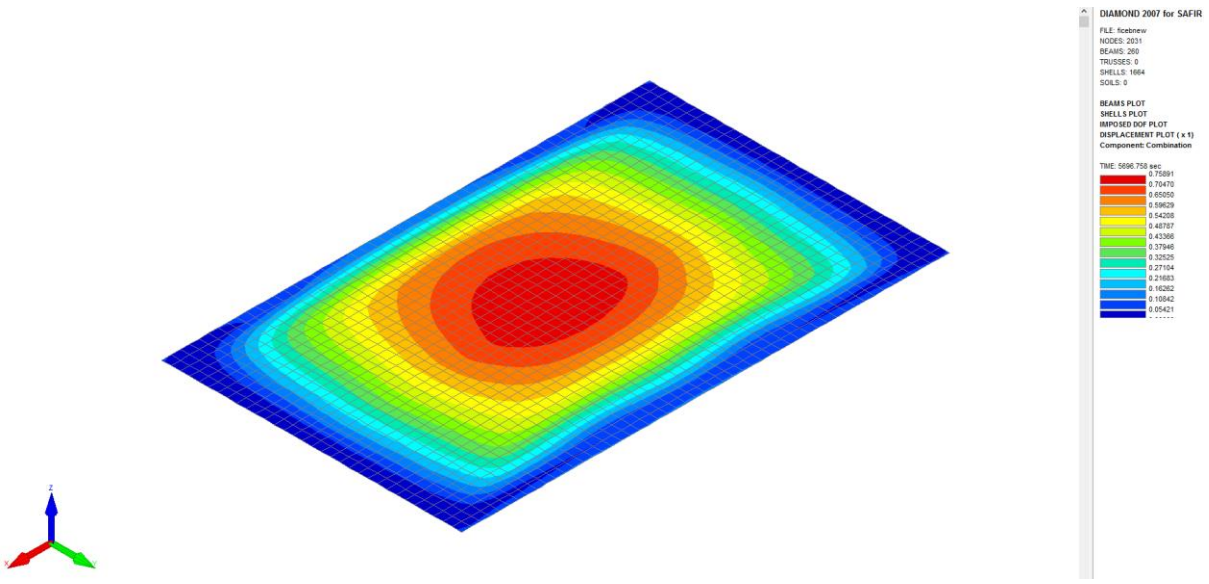

Fig. 4.3.4.5. Deflections of the slab (maximum)

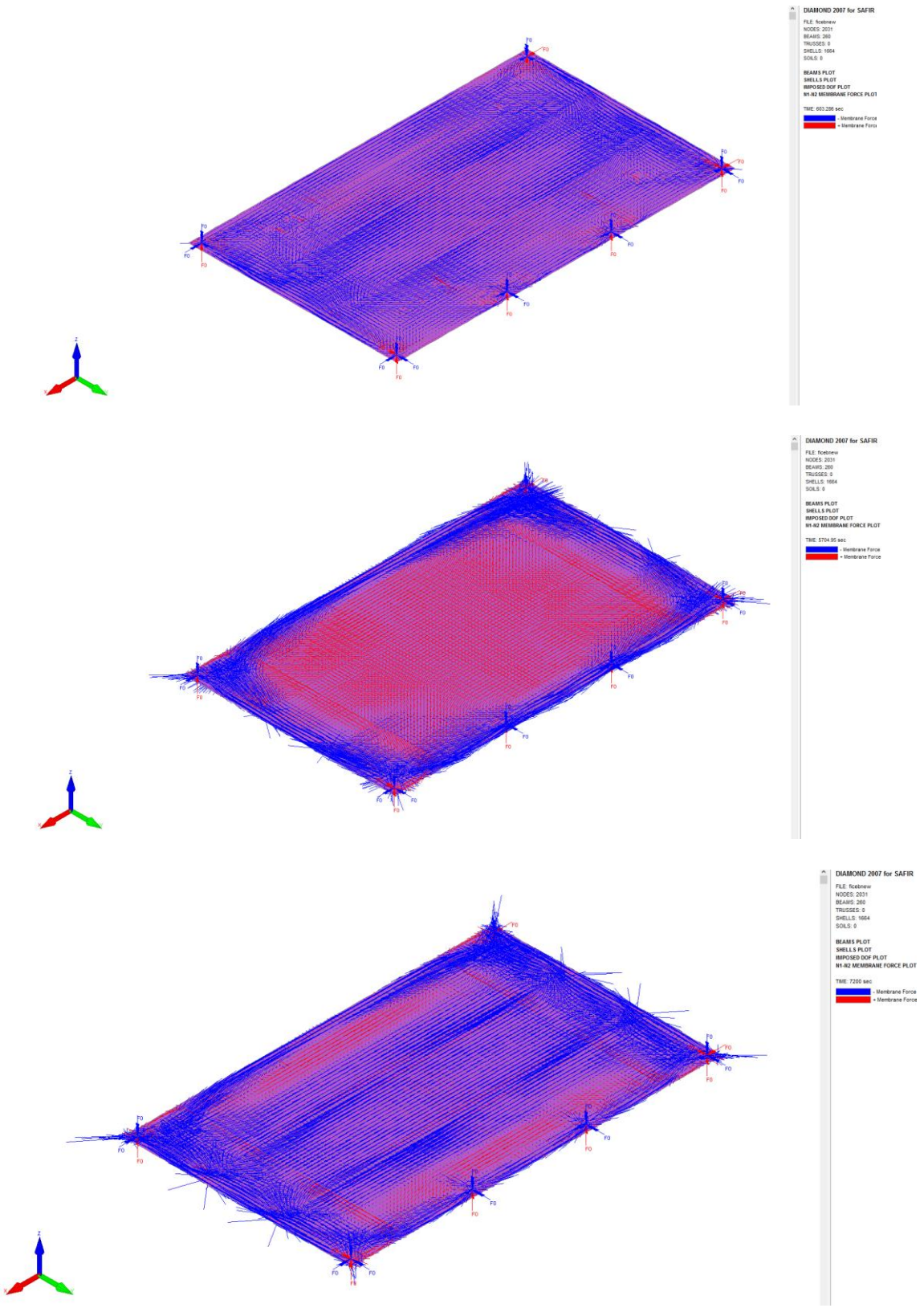

Fig. 4.3.4.6.a-c. Membrane action at: a) 10 min; b) 95 min; c) 120 min

4.3.5 POST-BUCKLING BEHAVIOUR OF UNPROTECTED BEAMS

During the fire test, the unprotected beams have moved towards each other, due to web-post buckling, even though the entire structure had not failed yet. This may suggest that the lower tee did not play any part in the global behaviour of the floor from this web-post buckling. Two simulations were considered:

1) In the first simulation, the steel stress-strain curves given in EN 1994-1-2 (2005) are used for both tees of the unprotected beams (see Fig. 4.3.5.1);

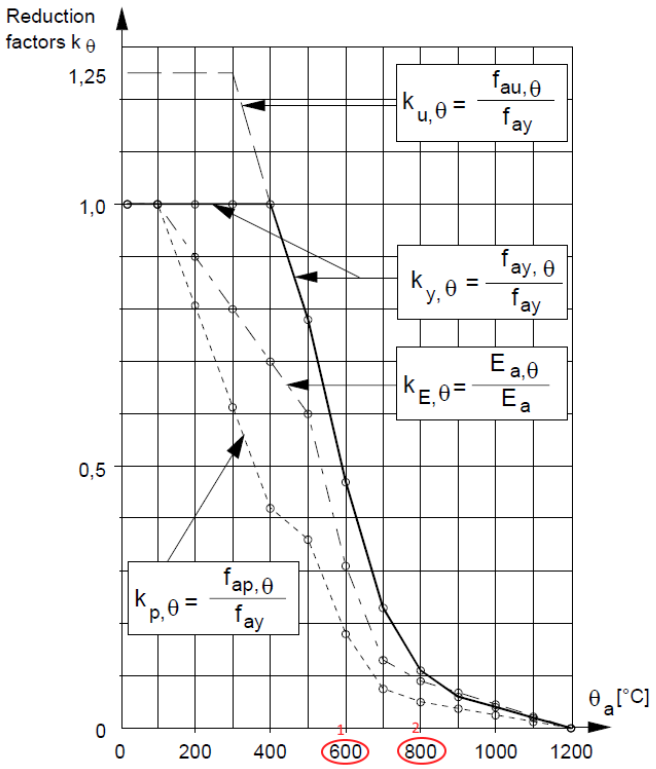

Fig. 4.3.5.1. Reduction factor for steel according to EN 1994-1-2 (2005)

2) In the second simulation, curves from EN 1994-1-2 (2005) are used in the upper tee. In the lower tee, the steel reduction factors are reduced to 1/1000th of their actual values from the point it reaches certain temperature to the end of

the simulation, including cooling phase. This irreversible loss of strength aims at checking whether it is reasonable to neglect the contribution of the unprotected lower tees to the global strength of the structure once they reach a given temperature. Two cases were considered: 600°C (as in the previous attempt Fig. 4.2.2) and 800°C.

4.3.6 PROPERTIES OF FIRE PROTECTION FOR EDGE BEAMS

Contrary to the similar thermal distribution unprotected and simulated beams (see Fig. 4.3.6.1) temperature in protected beams showed high differences in comparison to the measured values. For the protected sections, the insulation material was given in the RFCS report (FICEB, RFCS, 2012) as 20mm spray vermiculite-cement for the cellular beams, while a 20mm board siliceous fibre was used for the solid section. The materials have constant thermal properties, which are for the vermiculite: thermal conductivity: 0.12[W/mK]; specific heat: 1100[J/kgK]; specific mass: 550[kg/m³]; moisture content: 16.5[kg/m³]; convection coefficient on hot surfaces: 35[W/m²K]; convection coefficient on cold surfaces: 4 [W/m²K]; relative emissivity : 0.8[-] (as considered in the previous simulation of the test given in the RFCS report FICEB, 2012).

The thermal properties of the board siliceous fibre are: thermal conductivity: 0.15[W/mK]; specific heat: 1200[J/kgK]; specific mass: 600[kg/m³]; moisture content : 18[kg/m³]; convection coefficient on hot surfaces: 35[W/m²K]; convection coefficient on cold surfaces: 4[W/m²K]; relative emissivity : 0.8[-] (as considered in the previous simulation of the test given in given in the RFCS report FICEB, 2012).

However, these properties allows edge steel beams to heat up more than 500°C under ISO fire within 2 hours – the fire resistance time for which the slab was designed for. Thus, considering these values for the insulation properties (the most important being the thermal conductivity and the specific heat, which normally are not constant under elevated temperatures), lead to unrealistic high temperatures on the cross-sections, and thus to higher displacements of the slab edges.

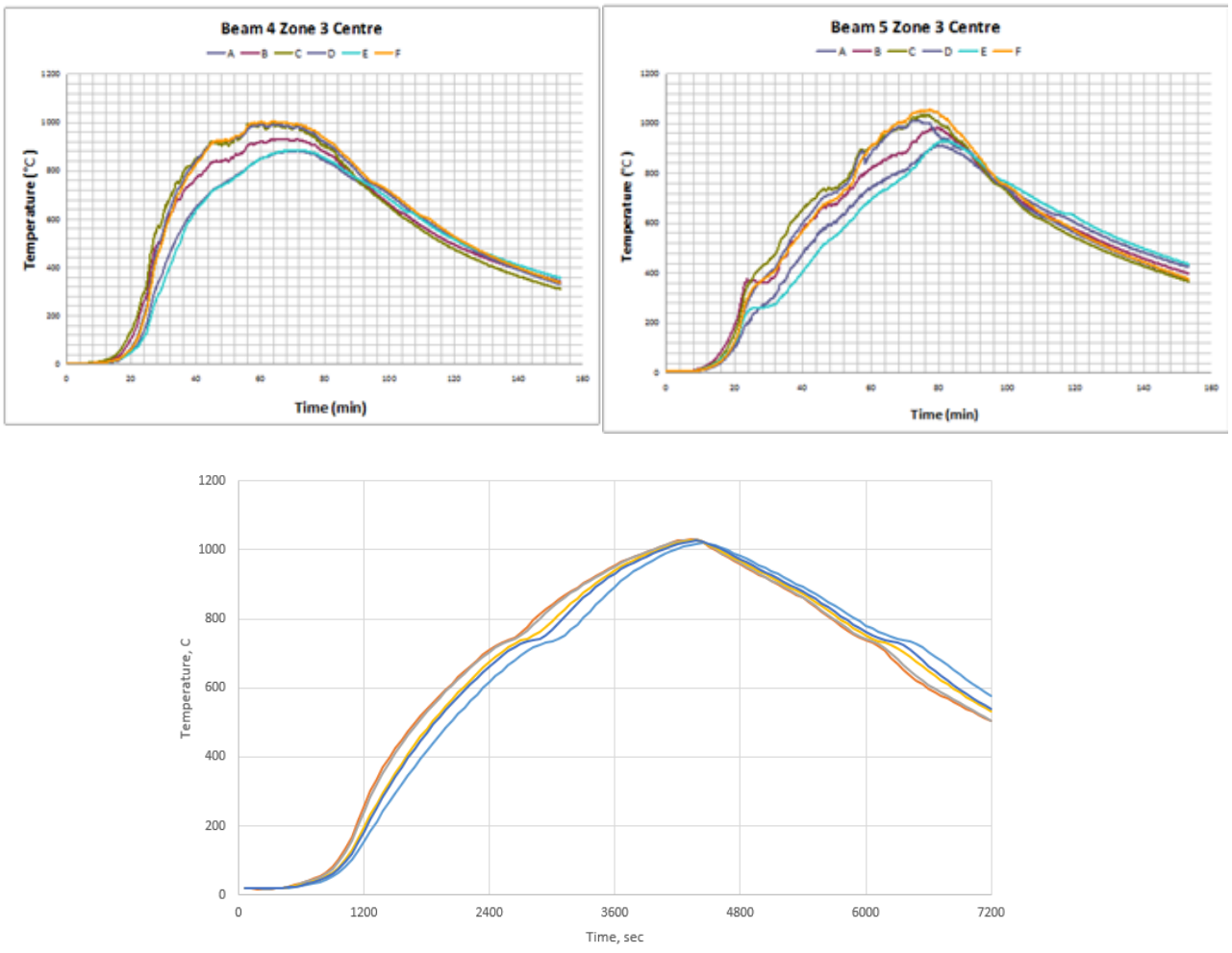

Fig. 4.3.6.1. Thermal distribution in the unprotected beams (MACS+, RFCS, 2014)

A first calibration may be done under ISO fire conditions (as this structure supposed to survive at least 2 hours of ISO fire) by imposing the condition that

the maximum temperature should not exceed 500 °C. The calibrated thermal conductivity value could be then used for natural fire simulation.

In case to have correct temperature distribution curves Fig. 4.3.6.2-4 thermal conductivity of protection layer was reduced to 0.04 W/mK.

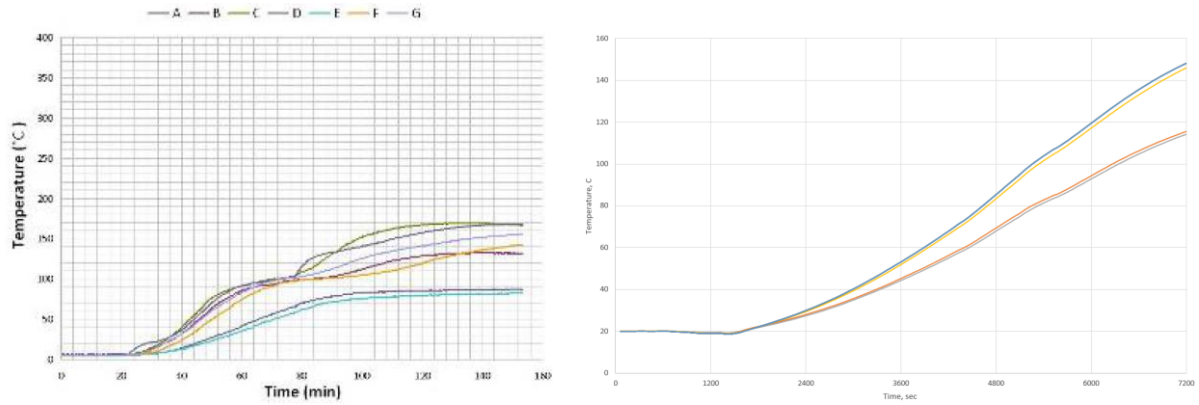

Fig. 4.3.6.2. Temperature at protected cellular beam (1) measured and modelled (FICEB, RFCS, 2012)

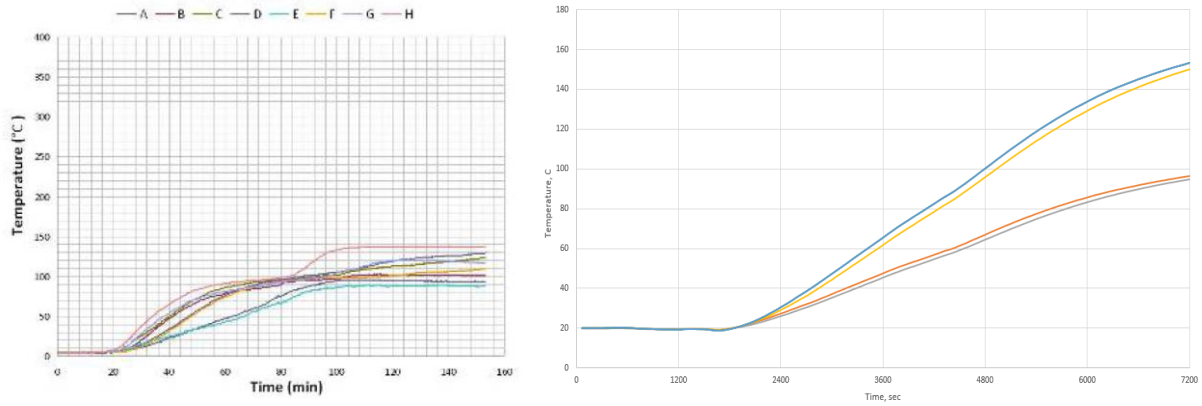

Fig. 4.3.6.3. Temperature at protected cellular beams (2) measured and modelled (FICEB, RFCS, 2012)

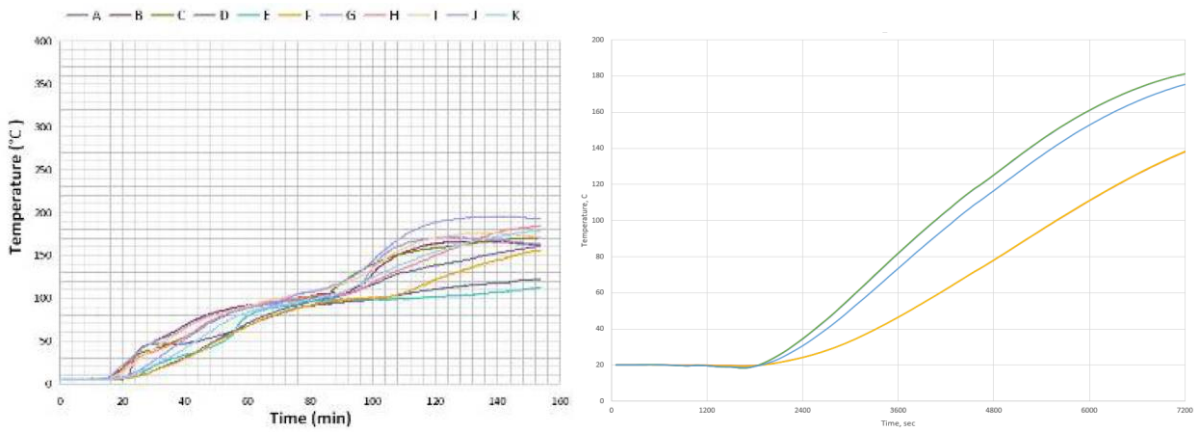

Fig. 4.3.6.4. Temperature at protected solid beam (3) measured and modelled (FICEB, RFCS, 2012)

CHAPTER 5.

RESULTS OF THE NUMERICAL SIMULATION

5.1 SOLID UNPROTECTED SECTION UNDER EXACT FIRE

In a first simulation, the whole section (see Fig. 5.1.2) of unprotected cellular beam was considered, with "exact" fire load (see Fig 5.1.1).

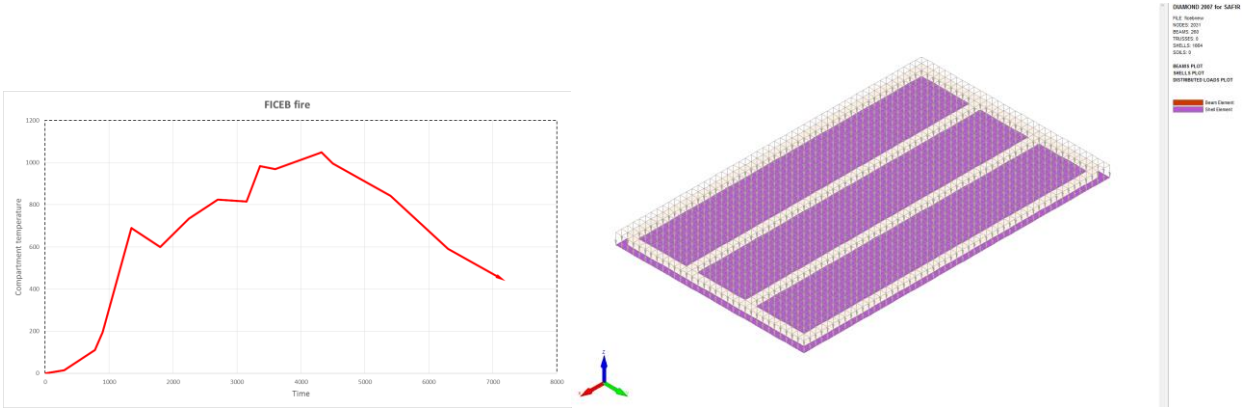

Fig. 5.1.1. Exact fire load and distributed imposed load

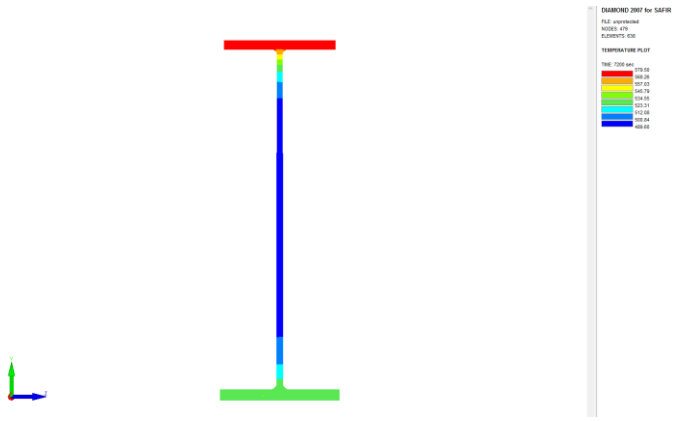

Fig. 5.1.2. Thermal distribution inside solid cross-section

Fig. 5.1.3 shows the comparison between the measured and computed vertical deflection at the middle of the unprotected beam.

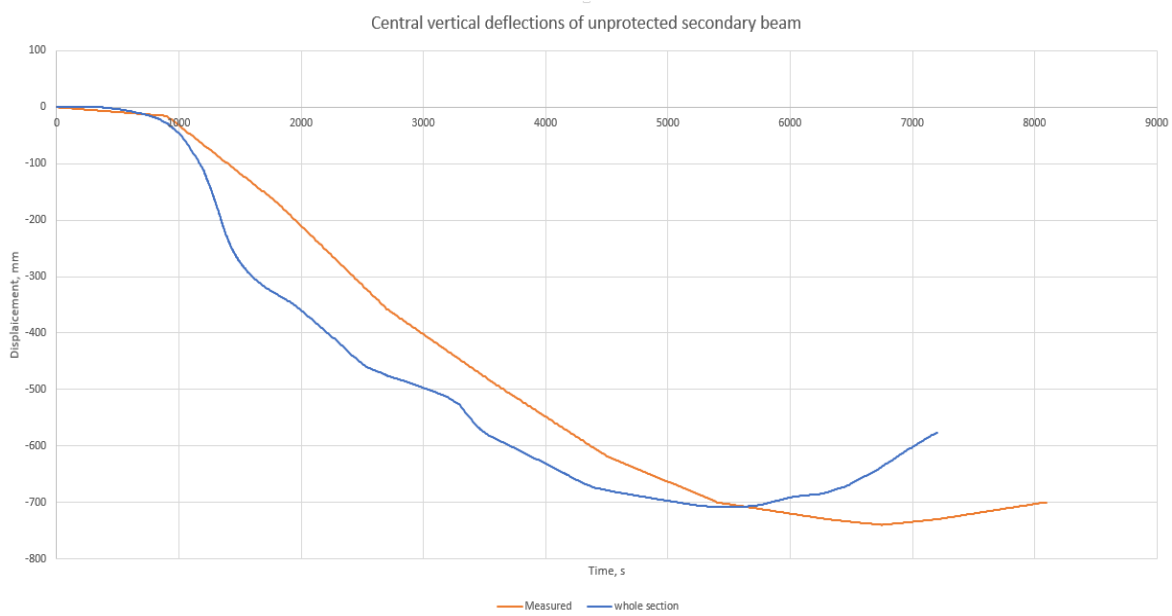

Fig. 5.1.3. Comparison between measured and computed vertical deflection at the middle of the unprotected beam

5.2 MINIMAL SECTION UNDER EXACT FIRE

With the same conditions as before, the geometry of the unprotected cellular beam was changed (see Fig. 5.2.1). The results are shown in Figure 5.2.2.

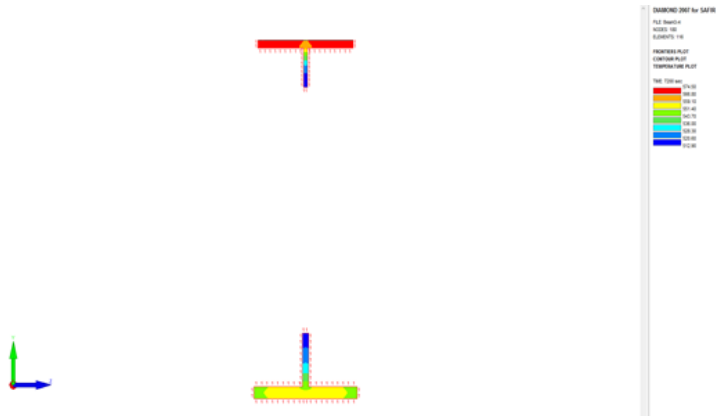

Fig. 5.2.1. Thermal distribution inside double tee cross-section

The vertical deflection in this case is closer to the measured one, but still not on the safe side.

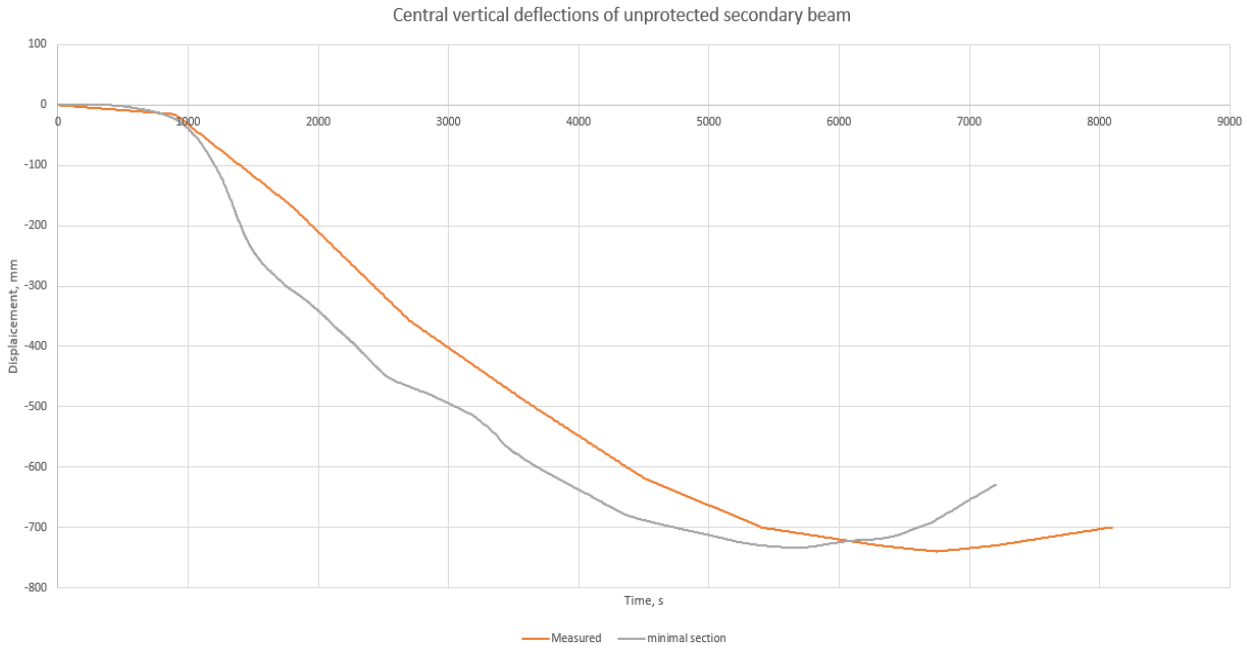

Fig. 5.2.2. Comparison between measured and computed vertical deflection at the middle of the unprotected beam

5.3 MINIMAL SECTION WITH DIFFERENT FIRES

Using the same geometry and smoothed fire load for unprotected beams as well as for the slab, fire applied to the protected edge beams was changed (see Fig. 4.3.1.5).

The results obtained in this simulation showed that with decreasing temperature inside the edge beam (and strengthening of this beams accordingly) the deflection decreases (see Fig. 5.3.1).

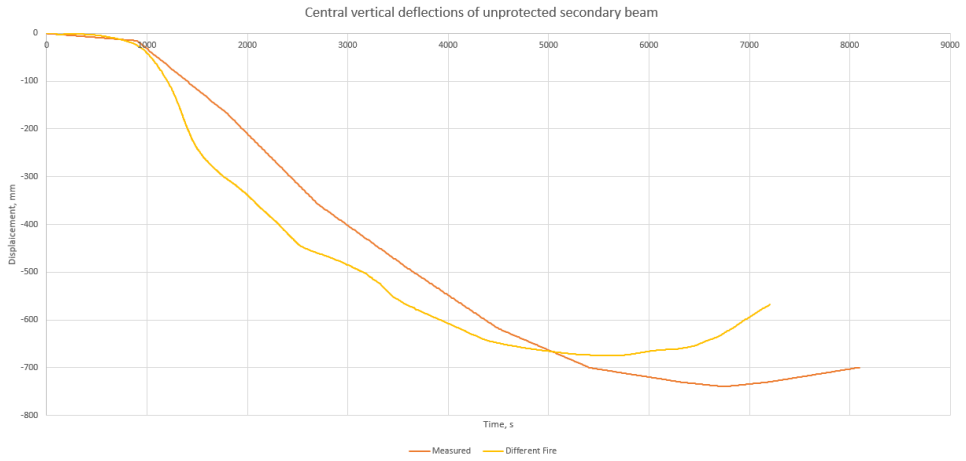

Fig. 5.3.1. Comparison between measured and computed vertical deflection at the middle of the unprotected beam

5.4 POST BUCKLING OCCURS AT 600 °C

In case of assuming the loss of carrying capacity of steel in lower tee section at 600 °C (see Fig. 5.4.1) it is necessary to create a new USER_STEEL material in SAFIR and follow the procedure describe in section 4.3.5.

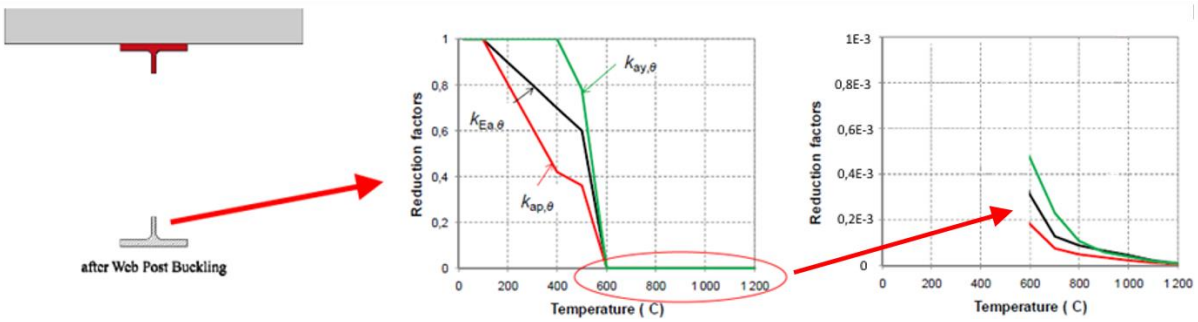

Fig. 5.4.1. Post buckling behaviour of the lower flange in the unprotected beam (FICEB, RFCS, 2012)

As Figure 5.4.2 shows, the loss of the lower tee after 600°C does not represent in a very precise manner real behaviour of structure. However, in this case, the value of the maximum displacement is on the safe side.

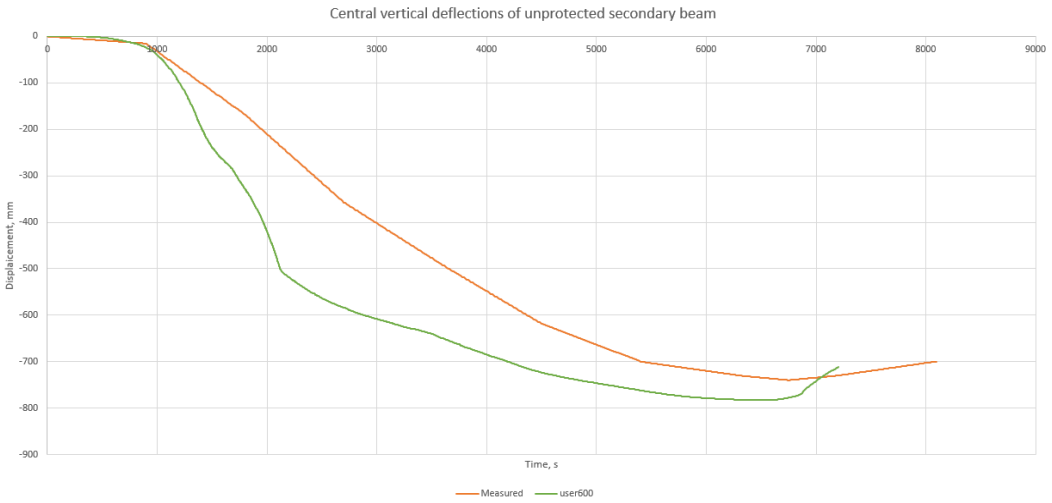

Fig. 5.4.2. Comparison between measured and computed vertical deflection at the middle of the unprotected beam

5.5 POST BUCKLING OCCURS AT 800 °C

The procedure is the same as in the previous case, but now after 790 °C the steel reduction factor will decrease 1000th times until 810 °C. It means that around 800°C, the lower tee section is "out" from the structural model.

As shown in Figure 5.5.1, this assumption verified experimentally by Vasart and Zhao (ECCS, 2013) leads to the closest structural behaviour in comparison with the test and has the maximum displacement value not only on the safe side but also very close to the measured one.

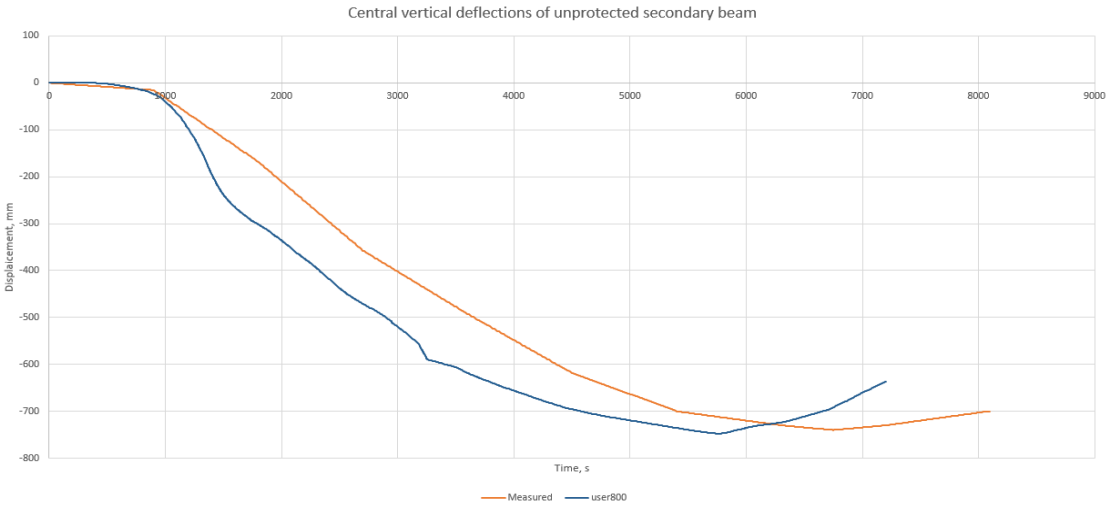

Fig. 5.5.1. Comparison between measured and computed vertical deflection at the middle of the unprotected beam

This simulation showed the closest behaviour in comparison with the test.

Consequently, it may be concluded that, the most simple numerical model which represents best the real full scale natural fire test is the one for which the following assumptions/ parameters were considered:

- Primary and secondary beams have been idealized using BEAM elements, and the slab using SHELL elements;
- Instead of ribbed cross-section, equivalent thickness of the slab has been used according to EN1994-1-2. Annex D (2005);
- Introduction of different fire cureves to different elements were done;
- Properties of fire protection for edge beams were calibrated;
- The loading was assumed as a distributed along the slab;
- Minimal section without the slab above, was used for thermal analysis;
- Post buckling occurs rapidly around 800 °C.

5.6 THERMAL CONDUCTIVITY OF CONCRETE

As in the test report it is not specified which value should be considered in fire conditions for the thermal conductivity of concrete (EN 1992-1-2 (2005) mention a maximum and a minimum value) both critical cases – minimum and maximum - were checked.

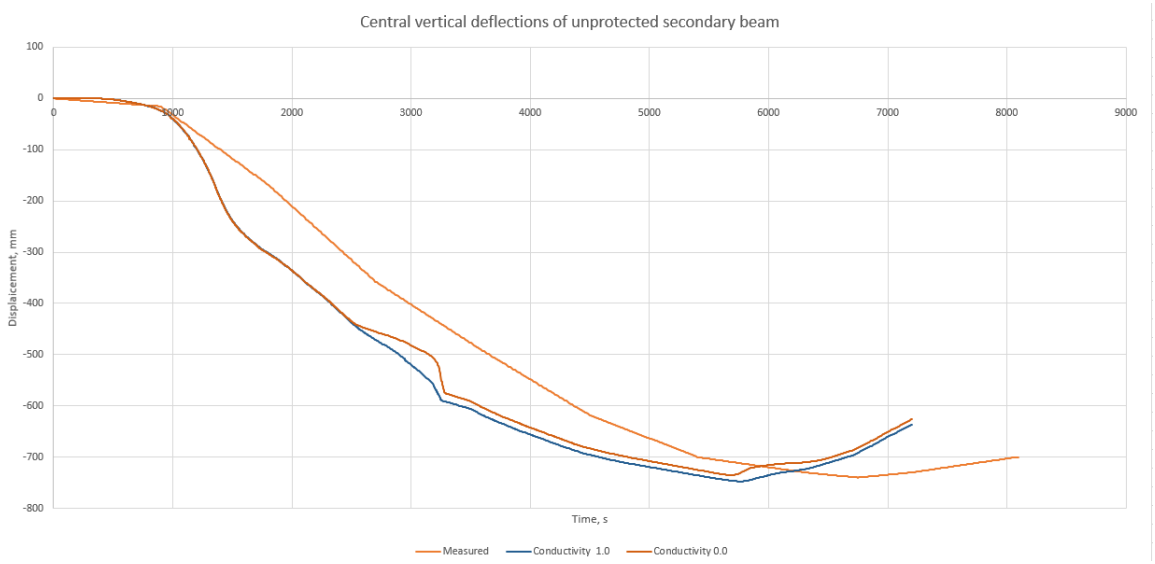

Fig. 5.6.1. Comparison between measured and computed vertical deflection at the middle of the unprotected beam

As it may be seen from Fig. 5.6.1, the influence of this parameter is insignificant.

5.7 OBSERVATION OF SIMPLIFICATIONS USED FOR FICEB TEST

Together with the simplifications which were considered before (see Section 2.3), new cases were also studied.

5.7.1 USING COMPOSITE SLAB FOR THERMAL ANALYSIS

It is not really necessary to consider the influence of the concrete slab above the beam cross-section, in the thermal analysis of the steel beams (both protected and unprotected), as mentioned in (MACS+, RFCS, 2014), (FICEB, RFCS, 2012), as it does not have a very strong influence on the thermal and structural behaviour of the member. On the other hand, if the presence of the slab is neglected, this would lead to higher temperatures on the upper T and thus to results in the safe side (apart of the fact that the numerical model is simpler).

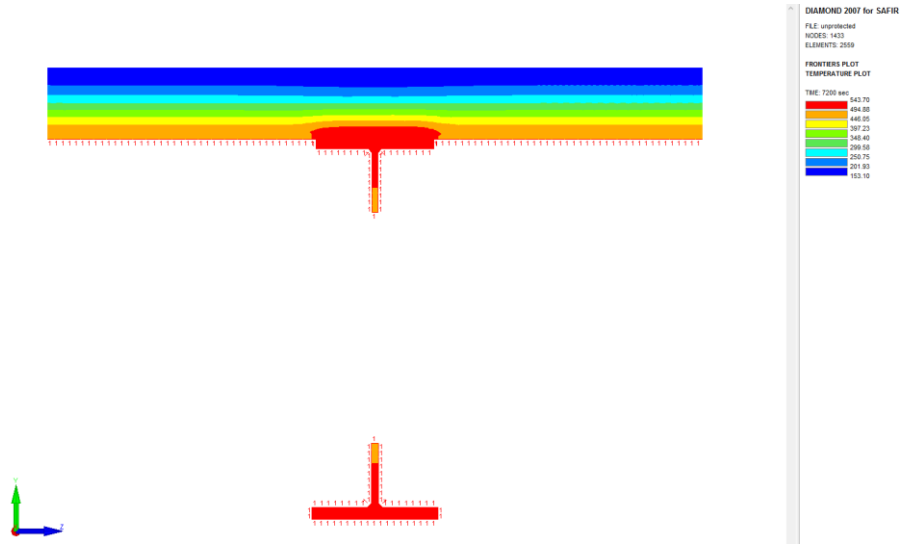

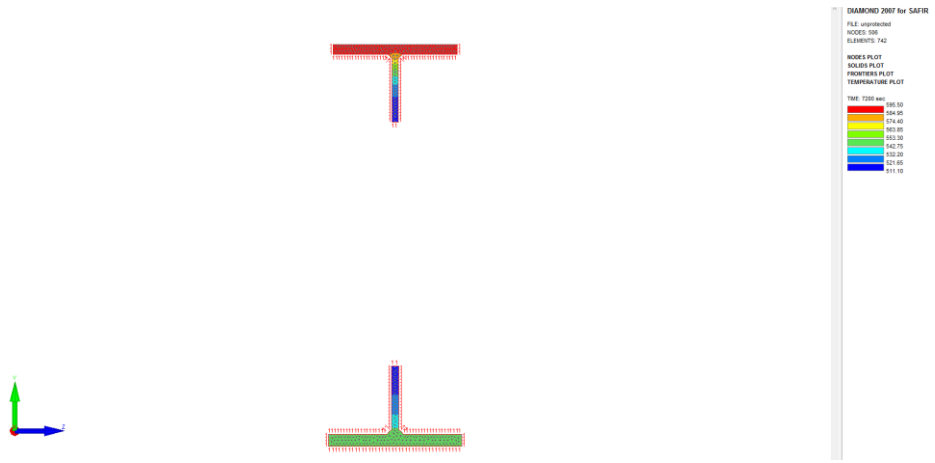

Fig. 5.7.1. Cross-section of unprotected beam with and without the slab above

For the actual FICEB numerical model, the maximum difference in terms of temperature is around 40-50 °C between the two cases, as shown in Fig. 5.7.2.

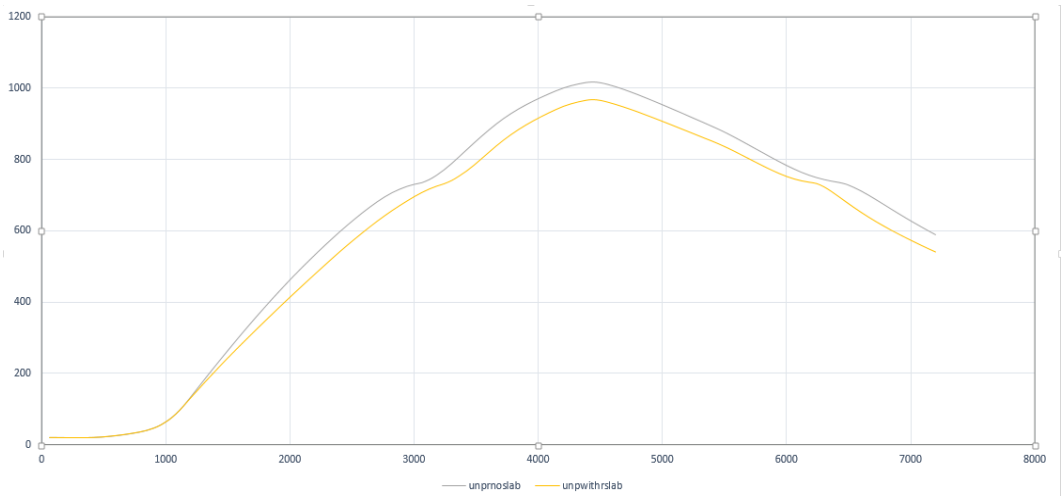

Fig. 5.7.2. Temperature distribution in the cross-section with and without slab above

In the protected beams (Fig. 5.7.3) this difference is even smaller (see Fig. 5.7.4).

Fig. 5.7.3. Cross-section of protected beam with and without the slab above

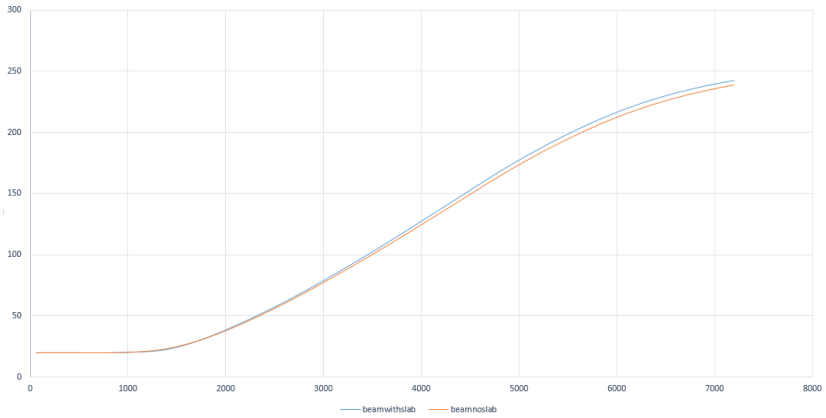

Fig. 5.7.4. Temperature distribution in the cross-section with and without slab above

5.7.2 SMOOTHING FIRE CURVE

Smoothing or not the natural fire curve has not a big influence, as Figures 5.7.5-6 demonstrate.

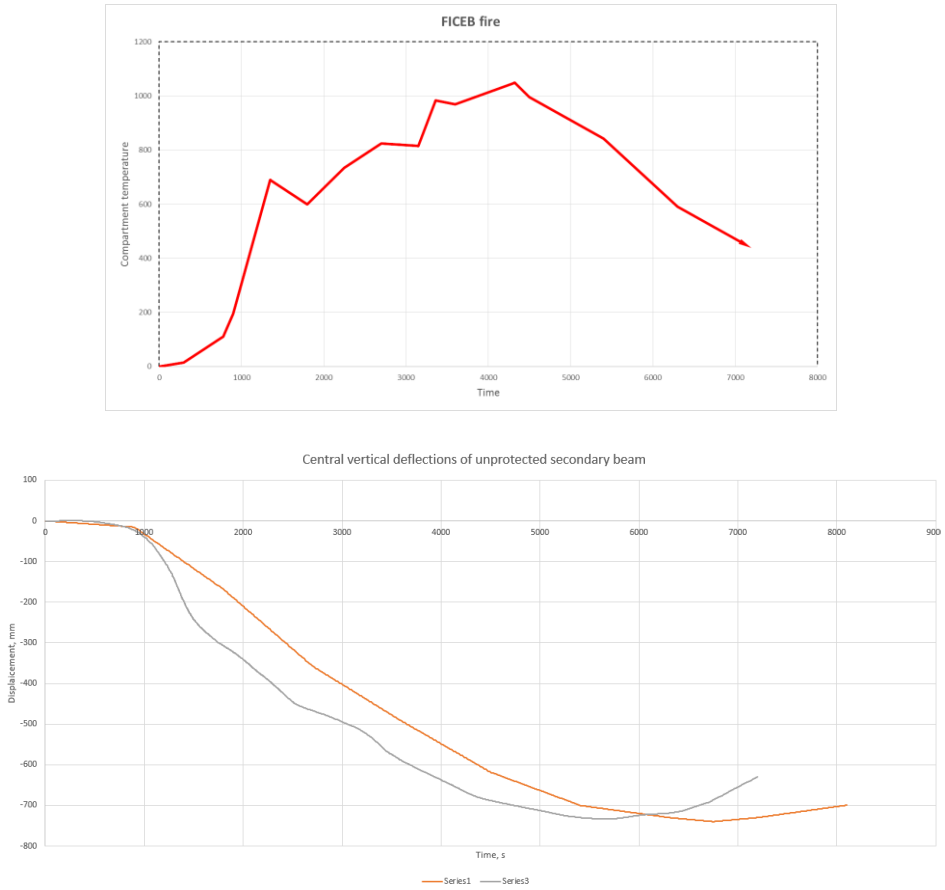

Fig. 5.7.5. Comparison between measured and computed vertical deflection under exact fire load

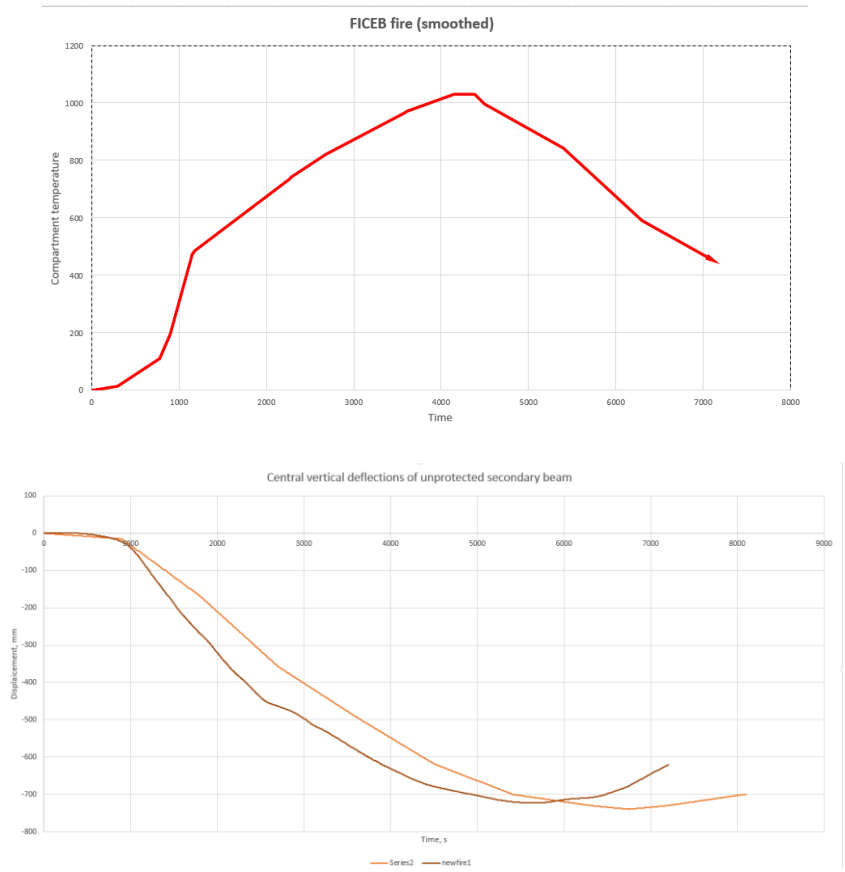

Fig. 5.7.6. Comparison between measured and computed vertical deflection under smoothed fire load

5.7.3 CONCENTRATED VS DISTRIBUTED LOAD

Considering concentrated loads instead of a uniform distribution of the loads (see Fig. 5.7.7-8) in order to follow real loading pattern created by the sand bags used in the test, gives close results. Therefore, it was concluded that for further simulations, to use the distributed load, which also offers results in the safe side.

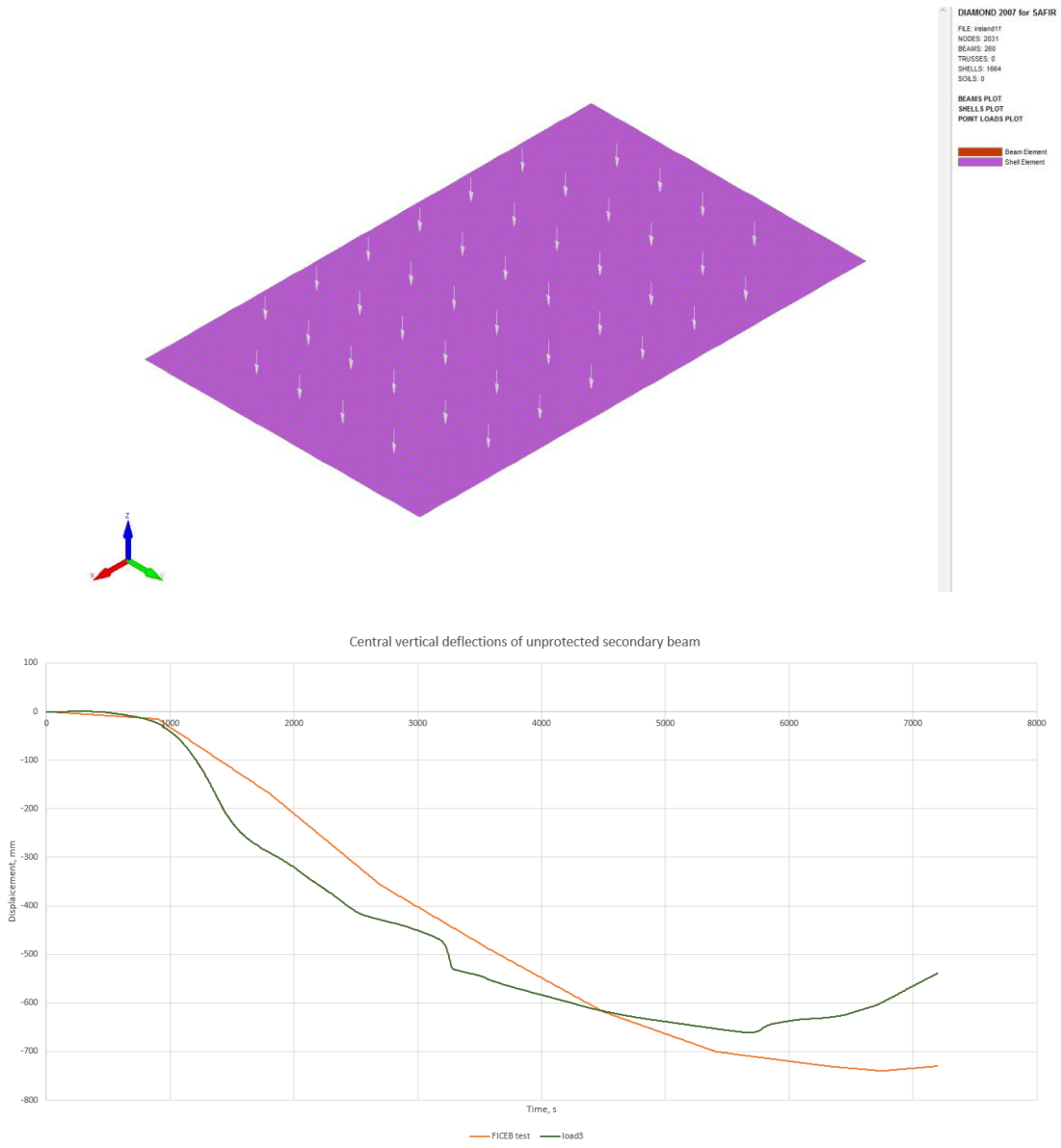

Fig. 5.7.7. Comparison between measured and computed vertical deflection under pointed load

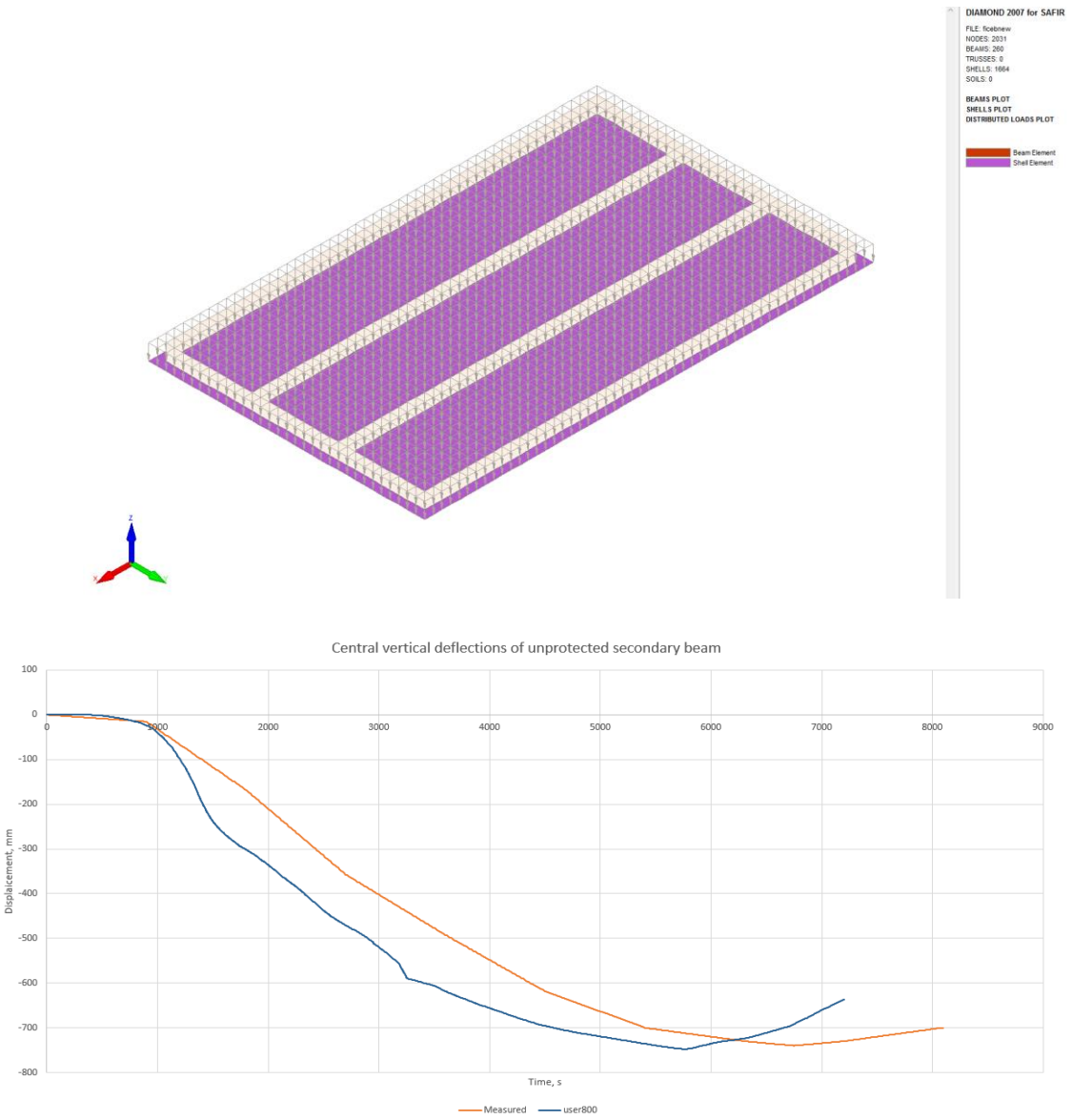

Fig. 5.7.8. Comparison between measured and computed vertical deflection under distributed load

5.8 STRUCTURE UNDER ISO FIRE

In order to check the correctness of numerical model (with the closest behaviour in comparison with the test) an analysis was run under ISO fire.

Within the numerical analysis it was assumed that the protected beams lost their insulation at 90 minutes (which would mean a target of 90 minutes of ISO fire resistants for the slab).

Assumptions used for the numerical model:

- Primary and secondary beams have been idealized using BEAM elements, and the slab using SHELL elements;
- Instead of ribbed cross-section, equivalent thickness of the slab has been used according to EN1994-1-2. Annex D (2005);
- Properties of fire protection for edge beams were calibrated;
- The loading was assumed as a distributed along the slab;
- Minimal section without the slab above, was used for thermal analysis;
- Post buckling occurs rapidly around 800 °C.

As shown in Figure 6.1, ISO fire loading leads to the failure of the structure at 92 minutes, which demonstrates that the numerical model is consistent with the assumption of 90 minutes of standard ISO fire resistance.

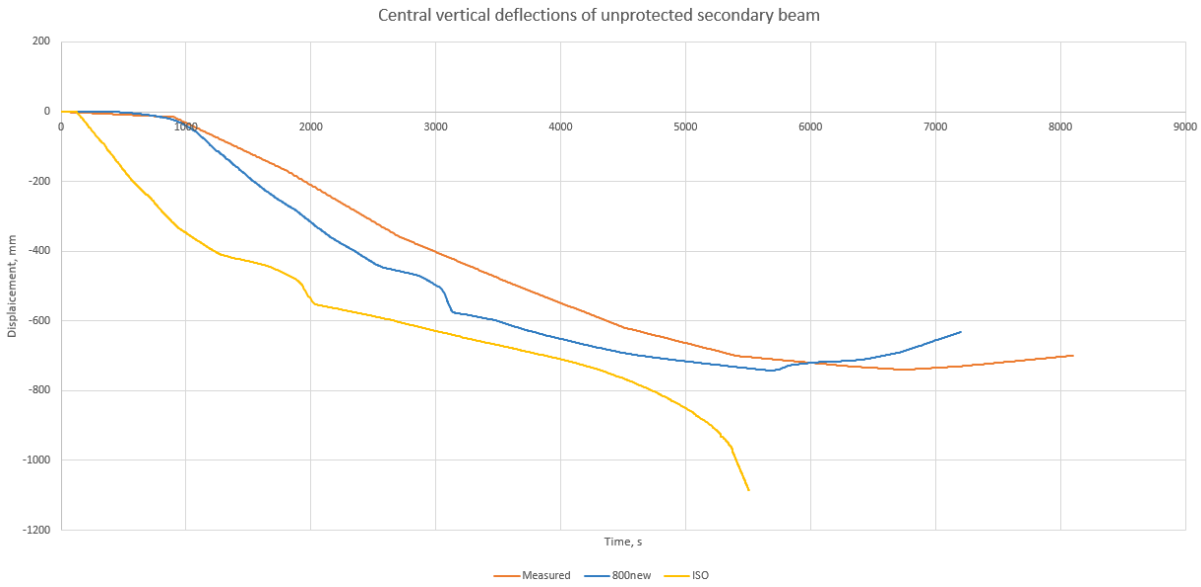

Fig. 6.1. Comparison between measured and computed vertical deflection at the middle of the unprotected beam

CONCLUSION

Using information from a real scale natural fire test, a number of numerical simulations were performed on a composite steel-concrete slab with cellular steel beams, by means of SAFIR program.

Based also on the experience obtained on numerical simulations on similar slabs tested under ISO fire (with solid steel beams) and on a previous simulation of the considered natural fire test, the work done within this thesis was aimed to propose a numerical model as simple as possible that, based on approximations, would nevertheless yield an appropriate representation of the structural behaviour and a safe estimation of the load bearing capacity.

The objective of the thesis was attained, the simplified numerical model considered (see Section 5.5) demonstrated a structural behaviour that is very close to the one observed experimentally.

In order to check the correctness of numerical model with the closest behaviour in comparison with the test, an analysis was also run under ISO fire. Within the numerical analysis it was assumed that the protected beams lost their insulation at 90 minutes (which would mean a target of 90 minutes of ISO fire resistance for the slab). The ISO fire leads to the failure of the structure at 92 minutes, which demonstrates that the numerical model is consistent with the assumption of 90 minutes of standard ISO fire resistance.

REFERENCES

1. EN 1992-1-2 (2005), "Eurocode 2 – Design of concrete structures. Part 1-2. General rules – Structural Fire Design", CEN, Brussels.
2. EN 1993-1-2 (2005), "Eurocode 3 – Design of steel structures. Part 1-2. General rules – Structural Fire Design", CEN, Brussels.
3. EN 1994-1-2 (2005), "Eurocode 4 – Design of composite steel and concrete structures. Part 1-2. General rules – Structural Fire Design", CEN, Brussels.
4. Zaharia R., C. Vulcu, O. Vassart, T. Gernay, Franssen J.M. (2013). "Numerical analysis of partially fire protected composite slabs". Steel and Composite Structures. 14(1). ISSN 1229-9367
5. Franssen, J.M. (2007), "User's manual for safir 2007 a computer program for analysis of structures subjected to fire", University of liege, Department ArGEnCO
6. Franssen, J.M. (2005), "SAFIR – A thermal/structural program modelling structures under fire", Eng J Aisc, 42(3), 143-158.
7. Vassart O., Hawes M., Simms I., B. Zhao, J.-M. Franssen, A. Nadjai,Research Fund for Coal and Steel (RFCS) (2012), Contract No RFSR-CT-2007-00042: "Fire resistance of long span cellular beam made of rolled profiles (FICEB)", 250
8. Vassart O., Zhao B. (2013), "Membrane Action of Composite Structures in Case of Fire", ECCS TC3 Fire Safety, 247
9. Vassart O., Zhao B., Hamerlink R., Hauke B., J. de la Quintana, I. Talvik, Sokol Z., Pustorino S., Vila Real P., M. Hawes, A. Nadjai, B. Åstedt, K. Jarmai, Zaharia R. D., Kvedaras A. K., C. Baniotopoulos, D. Beg, Franssen J. M., Wozniak G. (2014), "Membrane action in fire design of composite slab with solid and cellular steel beams — valorisation (MACS+)", RFCS Grant Agreement RFS2-CT-2011-00025, Final report

10. Vulcu, C., Gernay, Th., Zaharia, R. and Franssen, J.M. (2010), "Numerical modelling of membrane action of composite slabs in fire situation", Proceedings of 6th Intl Conference Structures in Fire, East Lansing, USA.
11. Vulcu M. Cristian (2009), "Numerical Modelling of Membrane Action of Composite Slabs in Fire Situation", UPT.
12. COSSFIRE (2006), "Connection of Steel and Composite Structures Under Natural Fire Conditions", RFCS research project N° RFSR-CT-2006-00028.
13. Bailey, C.G. (2001), "Steel structures supporting composite floor slabs: design for fire", BRE Digest, 462
14. Bailey, C.G., Lennon, T. and Moore, D. B. (2003), "The behaviour of a multi-storey composite steel framed building in fire", Struct Eng, 81/2, 27-36.
15. Bailey, C.G. (2004), "Membrane action of slab/ beam composite floor systems in fire", Eng Struct, 26, 1691-1703.
16. Zhao, B., Roosefid, M. and Vassart, O. (2008), "Full scale test of a steel and concrete composite floor exposed to ISO fire", Proceedings of the 5th International Conference on Structures in Fire SiF'08, Singapore City, Singapore, May.
17. Cadorin, J.F., Pintea, D., Dotreppe, J.C. and Franssen, J.M. (2003), "A tool to design steel elements submitted to compartment fires – OZone V2. Part 2: Methodology and application", Fire Safety J, Elsevier, 38, 429-451.
18. Li, G.Q., Guo, S.X. and Zhou, H.S. (2007) "Modelling of membrane action in floor slabs subjected to fire", Eng Struct, 29, 880-887.
19. SCI - Swinden Technology Centre (1999), 'The behaviour of Multi-storey steel framed buildings in fire – A European joint research programme", British Steel, Rotherham, U.K.
20. Wang, Y.C. (1996), "Tensile membrane action in slabs and its application to the Cardington tests", Second Cardington Conference, BRE, Watford, UK.

21. Yin, Y.Z. and Wang, Y.C. (2006), "Analysis of behaviour of steel beams with web openings at elevated temperatures", Steel Compos Struct, 6(1), 22-32.
22. Wald, F., Chladna, M., Moore, D., Santiago, A. and Lennon, T. (2006), "Temperature distribution in a full-scale steel framed building subjected to a natural fire", Steel Compos Struct, 6(2), 159-182.
23. 'Fire Safe Design: A new approach to multi-storey steel framed buildings' P288, The Steel Construction Institute, 2006.
24. MT ACB+ : ArcelorMittal Cellular Beams – CTICM Report 7.072-01